BAW-138

CONSOLIDATED EDISON THORIUM REACTOR
CONTROL SYSTEM DESIGN

August 1960

By
W. E. Carson
W. B. Chubb
R. T. Pickett
J. C. Deddens

Approved by: *B A Mong*
B. A. Mong
Chief,
Reactor Engineering

Approved by: *W C Gumprich*
W. C. Gumprich
Manager,
Engineering Department

PREPARED FOR
THE CONSOLIDATED EDISON COMPANY OF NEW YORK
BY

THE BABCOCK & WILCOX COMPANY

ATOMIC ENERGY DIVISION

Lynchburg, Virginia

CROSS REFERENCE INDEX

This Cross Reference Index has been prepared to key the supplementary material to the information which is contained in the Hazards Summary Report dated January, 1960, Exhibit K-5 (Rev-1) filed with Amendment No. 10 to Consolidated Edison's Application for Licenses.

SECTION 2 - REACTOR DESIGN

5_3 006

CONTENTS

LIST OF TABLES

LIST OF FIGURES

ABSTRACT

The Consolidated Edison Thorium Reactor Control System has been designed to provide the operators with a reliable, safe and accurate means of controlling the plant. Manual and automatic positioning of control rods can be accomplished. The automatic plant controller has been designed to meet the design criteria under the representative CETR demanded load changes. Adaptability has been built into the plant controller by providing variable controller adjustments for variations in reactor characteristics. Extensive analog studies have been made of the various plant parameters and their effect on control was carefully evaluated. These analog studies have shown that the control system will perform in a satisfactory manner under the most adverse plant conditions.

I. INTRODUCTION

The Consolidated Edison Thorium Reactor (CETR) core is composed of 120 fuel elements. Twenty-one movable hafnium cruciform control rods interspersed on a square grid among the fuel elements furnish the means for automatic and manual adjustment of the reactor power level.

The CETR control system is designed to maintain constant steady state steam pressure regardless of steam demand. The maintenance of constant steam pressure independent of power level causes the average reactor coolant temperature to rise with increasing power level.

The CETR has a negative moderator temperature coefficient of reactivity which opposes an increase in moderator temperature and tends to drop steam pressure with increasing load. Another negative coefficient of reactivity, the fuel temperature coefficient (Doppler effect), opposes an increase in reactor power level.

Substantial reactivity changes are required when changing power level to force the necessary variation of average coolant temperature against the opposing action of the two negative reactivity effects mentioned. Reactivity adjustment is supplied by movement of control rods through the reactor control system.

The control system provides for programmed movement of groups of control rods, either automatically to match load demand, or manually at the discretion of the operator. Various groups of control rods must be removed in a predetermined sequence in order to insure against too severe localized power peaking in the reactor core. The control system automatically carries out this sequence through the sequence switching unit.

Mathematical models of the plant components were derived to arrive at the proper combination of control system parameters.

These models were then solved through the use of an electronic analog simulation of the plant and control system. Discrete points in the core lifetime were considered and the reactor control system requirements determined. The plant response characteristics to load demand changes were determined.

II. DESCRIPTION OF THE CONTROL SYSTEM

A. EQUIPMENT

1. Control Panels

Supervisory Panels

Instrumentation and controls for control rod drive
testing and for manual startup of the reactor and
for alternative manual operation of the reactor to
full power are located on certain Supervisory Panels.
Also located on these panels are the trend recorders
required to start and operate the plant as well as the
monitors, indicators, controls and alarms relating
to system auxiliary conditions and efficiency.

Flight Panel

Indicators, alarms and controls on the Flight Panel
together with trend recorders mounted on the Super-
visory Panels, permit the operator to manually or
automatically control the reactor from its low power
limit (5-15% of full load) to full load and to control
the remainder of the plant.

Sections of a Supervisory Panel and of the Flight Panel are used
for reactor control. Operations below a preset point adjustable between
5 and 15% power level must be controlled from the Supervisory Panel.
Manual operations above the preset point may be controlled from either
panel. Automatic operation during electric power generation must be
from the Flight Panel.

The major information affecting reactor control is displayed on
the two control panels as shown in Table I.

- 3 -

TABLE I
CONTROL PANEL-DISPLAYED INFORMATION

Supervisory Panel	Flight Panel
Reactor Period	Rod Group Position
Log Count Rate	Log Level
Log Level	Reactor Period
Individual Rod Position	Linear Power Level
Rod Group Position	Steam Flow and Pressure
Linear Power Level	Reactor Temperatures
	Automatic Control Demand Signal

2. Control System Operation

Any one of three conditions of reactor operation can be selected by positioning a selector switch on the Supervisory Panel. These conditions are identified as (1) STANDBY (2) START and (3) OPERATE.

STANDBY permits the manual positioning of all individual control rods, one at a time, or all groups of control rods, one group at a time, from only the Supervisory Panel for test, adjustment or core loading operations, provided the log count rate is above 5-10 CPS but below 10^{-6} full power. Individual rods move at the maximum rod velocity.

Any group of rods may be controlled directly or through the sequence switching unit described in Section 3. Selected speeds are fixed by manual speed control units associated with each group of rods.

START permits manual positioning of groups of control rods in a predetermined sequence by the sequence switching unit from the Supervisory Panel at any power level from a log count rate of 5-10 CPS to 100% power. Selected speeds are fixed by manual speed control units associated with each group of rods. Interlocks prevent operation in START unless safety conditions, such as minimum primary coolant temperature, have been satisfied and safety relay resets have been made.

OPERATE transfers control from the Supervisory Panel to the Flight Panel and permits manual or automatic operation of groups of control rods in a predetermined sequence at power levels above the preset minimum.

Manual-group control is through the sequence switching unit when the Supervisory Panel switch is in the OPERATE position and when steam flow is above a preset 5-15% full power steam flow.

Automatic-group control has as its primary function the automatic control of selected groups of rods, through the sequence switching unit, at speeds determined by the rod reactivity control system requirements. This mode of control is available only from the Flight Panel when the selector switch on the Supervisory Panel is in the OPERATE position and only when steam flow is above a preset 5-15% of full power steam flow. Rod groups are withdrawn or inserted under control of the sequence switching unit in accordance with the rod velocity demand signals received from the plant controller.

3. Equipment Functions and Operation

The control system is composed of the plant controller, rod programmer, and the control rod servomechanism. A functional block diagram of the control system is shown in Figure 1.

a. Plant Controller

The plant controller is used in Automatic-Group mode to control the reactor power output above 15% of rated power. Its functions are to maintain a constant steam pressure during steady state operation and to hold steam pressure variations within prescribed limits during power changes. Figure 2 is a functional block diagram of the plant controller. A steam flow signal is used to compute a reactor power demand signal, augmented by a steam pressure error signal. Two identical computing channels are provided, to duplicate functions. The two channels are compared automatically and an alarm is sounded and control automatically reverts to manual if the two differ by more than a preset amount. This minimizes the possibility of false rod velocity demand.

Steam pressure sensors in each of the four steam lines transmit pressure signals to averaging units in both channels. Each average pressure is compared to a reference pressure or set point. The outputs represent pressure error signals, ΔP, which are compared in a magnetic amplifier comparator. If these two signals differ, an alarm is sounded and control automatically reverts to Manual-Group

- 5 -

mode. The pressure error signals are transmitted to the gain plus reset until shown on Figure 2 to generate the following function:

$$N_P = K_2 \left[\Delta P + \frac{1}{\tau} \int \Delta P dt \right] \qquad (1)$$

Where

ΔP = steam pressure error signal

τ = reset time constant

K_2 = constant

Adjustments are provided to set the constants at desired values. Either channel 1 or 2 output may be selected to transmit to the totalizers. The totalizers add the steam flow signal as follows:

$$N_C = K_1 W_s + N_p \qquad (2)$$

Where W_s = steam flow signal

K_1 = constant

The output from the totalizers is the demanded power. A minimum power demand limit is set by the low limit bias supply unit. This prevents the power demand signal from demanding less than 15% of rated power. This lower limit is required to maintain reliable control since thermal and nuclear measurements are not accurate below that level. The power demand signal from the low limit bias supply unit, is limited by an average power level limit setting proportional to the coolant flow rate in the primary system. Individual comparators compare the demanded power with the actual reactor power as indicated by the Nuclear Instrumentation System. The outputs are power error computed as follows:

$$\epsilon_p = N_C - N_i \qquad (3)$$

Where N_C = demanded power

N_i = indicated power

The error signal then passes to a deadband unit, with the characteristics shown in Figure 3. The output of the deadband unit is the rod

- 6 -

velocity demand signal, $\dot{X}_d$. The rod demand signal is zero until the edge of the deadband is reached. A minimum rod speed of approximately 3 inches per minute may be called for. The demanded rod speed may increase up to a maximum of 22 1/2 inches per minute as the error increases. Both computing channels generate rod velocity demand signals, $\dot{X}_d$, which are compared in the velocity demand comparator magnetic amplifier. If an excessive difference occurs an alarm is sounded and control is automatically reverted to the Manual-Group mode. The rod velocity signal from either channel 1 or 2 is selected by the operator for transmission to the rod programmer and subsequently governs the movement of the control rod groups.

b. The Rod Programmer

The rod programmer consists of the group interconnection unit, the sequence switching unit and five group demand units. The input to the rod programmer is the rod velocity demand signal, $\dot{X}_d$, computed in the plant controller, or from the manual group control switches.

(1) Interconnection Unit

The CETR has 21 movable hafnium control rods. The rods are divided into four groups of four rods each and one group of five rods. Each group is assigned to a group demand unit which moves all rods of that group in unison.

The interconnection unit provides the means for assigning rods to the various group demand units. This is accomplished by a plug-in type patch board in which electrical leads to any four or five rods may be connected to a single group demand unit. These assignments are made by operating personnel prior to reactor start-up.

(2) Sequence Switching Unit

The assignment of rods to the five groups is determined on the basis of optimium power distribution in the reactor core. The five groups must also be removed from the core in a specified sequence to prevent localized overpeaking of the power in the core.

The sequence switching unit automatically carries out the sequence of rod removal which is set by the operator prior to start-up. The sequence switching unit routes the rod velocity demand signal

to one of the five group demand units which control the servo motor and control rod drive assemblies assigned to it. Only one group demand unit at a time receives the velocity signal. The sequencing is initiated by cams in the respective group demand units. When one group reaches its limit of travel control is automatically transferred to the next group. The sequence switching unit has a provision for allowing the operator to bypass any one of the groups in the automatic sequencing operation.

(3) Group Demand Unit

The group demand units generate the control rod position demand signal for each of the servo-controlled rod groups. A schematic of the group demand unit functions is shown on Figure 4. The input to the unit is a rod velocity demand signal either from the plant controller in automatic mode or from the operator in manual mode. The input is electrically limited to the maximum rod speed required for normal plant conditions. The synchronous speed of the integrator motor driving through a gear box inherently limits the speed should the electrical limitation fail.

The demanded rod velocity is received by the magnetic amplifier which in turn controls the speed of the velocity integrator motor shown on Figure 4. The output of the motor is proportional to the integral of the demanded rod velocity and is thus a rod position demand signal. The rod position demand is transmitted mechanically through gears and shafts to turn the rotors of three synchro transmitters. Two of the synchro transmitters transmit the position demand signal to the control rods servomechanisms assigned to that particular group demand unit. The third synchro transmitter is used to transmit a signal to the group position indicators on the Supervisory and Flight Panels.

Another mechanical connection to the velocity integrator motor is used to drive a tachometer which measures the actual velocity transmitted by the integrator motor. The actual velocity is then compared to the demanded velocity in a demand comparator. (See Figure 4.) If the two velocities differ by greater than a preset amount automatic control is discontinued and a velocity failure monitor sends a signal to the fast insertion network.

(4) Fast Insertion

Certain classes of failures are not serious enough to

- 8 -

warrant reactor scram. These are: the rod servomechanism velocity and position failure monitors, indicated reactor power exceeding 115% of full power, reactor period less than 20 seconds, control bus under-voltage, and turbine or superheater trip.

All of these failures, except a short reactor period when the reactor is below 0.1% full power, result in a signal to the fast insertion network. The fast insertion network energizes the control rod drive motors which drive all withdrawn rods into the reactor at the maximum speed of 22 1/2 inches per minute. This direct, or open loop, movement of control rods bypasses the group demand units and the sequence switching unit. The fast insertion motor shown on Figure 4 is used to restore the group demand unit to its starting position for open loop fast insertion.

During reactor start-up, when the operator is using the manual group mode of control, reactor periods of less than 20 seconds may be obtained. In this case the short period signal will cause insertion of the group of rods being withdrawn. Insertion takes place through the group demand unit, in proper sequence, and continues until the reactor period is again greater than 20 seconds.

c. Control Rod Servomechanism System

The control rods are positioned by individual servo loops through which each rod follows the group demand unit position demand signal. A schematic of the servo mechanism system is shown on Figure 5.

When the velocity integrator motor displaces the rotor of the synchro transmitter in the group demand units a position demand signal, X_d, is transmitted as a voltage to the position control transformer of the servo mechanism. (See Figure 5.) This voltage in turn induces a voltage across the rotor of the position control transformer proportional to the position error. The induced voltage from the control transformer rotor is amplified in a magnetic amplifier and causes a corresponding rotation of the rod drive motor. The rotational motion of the drive motor is translated to the linear motion of the rod through gears and lead screws.

A mechanical coupling exists between the rod drive motor and the control transformer rotor. The control transformer rotor is

- 9 -

turned as the drive motor rotates to restore the proper rotor-stator
orientation. The drive motor continues to move until the induced
voltage across the rotor is reduced to zero. When this occurs the
actual rod position corresponds to the demanded rod position. The
induced voltage from the control transformer rotor, is proportional to
the difference between actual rod position and demanded rod position.
This voltage is measured in a position failure monitor. If it exceeds
a preset amount a failure is indicated and all withdrawn rods are put
on open loop fast insertion.

A selsyn transmitter is driven by the rod drive motor shaft
to transmit individual rod position indication to selsyn receivers on the
Supervisory Panel.

B. THEORY

The previous section discusses the steps in computing the demanded
reactor power, N_C, (Eq. 2) and the rod velocity demand signal $\overset{\circ}{X}_d$. The
basis for the system is discussed in this section.

Reactor power level is made to match the demanded power from the
steam turbine and constant steam pressure is maintained through movement
of control rods. Control rod velocity, which is dependent upon the magnitude
of the power error signal (see Eq. 3), is demanded whenever the error
signal exceeds the power deadband. The deadband serves two functions.
(1) it minimizes control rod drive wear by eliminating unnecessary motion;
and (2) a small deadband is desirable to allow the inherent effects of the
temperature coefficients to make small adjustments in power level. Pre-
cise control is not desirable in a system with a long loop flow time because
overcontrol is likely to result with consequent tendency of the control
system to "hunt" and cause cycling of steam pressure.

The power demand signal is composed of three terms as shown in
Equations 1 and 2. These are (1) steam flow, W_s, (2) steam pressure
error, ΔP, and (3) integral of steam pressure error, $\int \Delta P dt$. The
greatest control effect is caused by the steam flow signal. This signal
is used to compute the demand which is proportional to a factor $K_1 W_s$
(see Eq. 2) (K_1 lies between 0.7 and 0.9.) This means that 100% steam flow
will demand 70% reactor power when K_1 is set at 0.7.[1] Steam pressure

---

[1] Values of 0.7 to 0.9 are normalized constants of the demanded power,
N_C, equation. The corresponding real values are listed in Table II.

error and the integral of steam pressure error are used to augment the steam flow signal and add the additional power demand of 30% of steady state demand. The integral term calls for more power when an error has been present for a length of time. The integral, or reset time, τ, is 200 seconds.

Variations in the control constants, K_1 and K_2, and the integral time, τ, have some effect on the plant control characteristics. Values of K_1 near unity will result in more rapid reactor response to steam demand but can cause excessive power overshoot. Power overshoot following all changes in power level is typical in a plant like the CETR with a long loop flow time and large thermal storage capacity. Accordingly K_1 is set between 0.7 and 0.9 for optimum performance under the control system design criteria. The pressure correction term, K_2, can also cause excessive overshoot if it is set too high. If K_2 is too low the length of time required to restore steam pressure to normal will be too long. Analog simulation studies indicate that values of the control constants can be chosen to give good recovery from transients without excessive power overshoot.

III. DESIGN CRITERIA

A. GENERAL

The basic criteria for plant operation are as follows:

1. Reactor power overshoot shall be limited to 10%.
2. Steam pressure for normal operation shall be maintained within a maximum variation of 60 psi.
3. Reactor period shall be greater than 20 seconds at all times during power operation.

B. LOAD CHANGE RATES

The required steam load rates of change are as follows:

1. 15 to 100% power at 53.2 MWt per minute (9.1% per minute)
2. 100 to 15% power at 53.2 MWt per minute
3. At 15% to 75% power, a step steam demand change equivalent to +106.4 MWt (18.2%)
4. At 30% to 75% power, a step steam demand change equivalent to -106.4 MWt (18.2%)

Where:

MWt = thermal megawatt, the unit of measurement used in describing the thermal output of the plant.

These steam load change rates were computed from an electrical load change requirement of 25 megawatt electrical per minute and a 50 megawatt electrical step, respectively. The corresponding steam load was computed as follows:

$$\frac{50}{275} \ (585 \ MWt) = 106.4 \ MWt \tag{5}$$

Where: 275 Megawatts electrical is full power plant output including the contribution from the separate oil fired superheater.

C. PLANT CHARACTERISTICS

The important parameters which affect the control system are load rate changes, fuel and moderator temperature coefficients of reactivity, water and steel masses, system flow times, and characteristics of the fuel rods. The general effects of the temperature coefficients were discussed in Section I, and the load rate changes were outlined in the previous section. The system flow time was mentioned briefly in Section II and will be discussed in more detail here. Water and steel masses and fuel rod characteristics are also discussed here.

1. Water and Steel Masses

The large masses of water and steel in the CETR primary loops contribute to the inertia of the plant and generally exert a stabilizing influence by reducing the magnitude of transients. In a constant steam pressure system the reactor must supply additional heat, above that required to match the load demand, to bring the primary masses to the new equilibrium temperature. This additional heat is supplied by forcing the reactor to overshoot temporarily the demanded power level. Conversely during decreasing load changes the primary masses contribute heat and the reactor power must be forced to undershoot temporarily the demanded power in order to allow reduction of the average primary mass temperature to the new equilibrium level.

2. System Flow Time

The system flow time causes a delay in transfer of heat from the reactor to the boilers when the steam load is increased. This time lag causes steam pressure to fall until the heat required from the reactor is available to counteract the change. Heat energy stored in the primary water partly offsets the steam pressure change by contributing heat immediately.

The reactor control system design parameters allow for the loop delay time and maintain steam pressure variations within the limits set forth in Section III.

3. Fuel Rod Characteristics

Several characteristics of the fuel rods exert an important influence on the control system design and plant response. The most

important of these are the low thermal conductances of the fuel pellets
and the gas filled gap which exists between the fuel pellet and the cladding.
The gas gap presents a high resistance to heat flow and therefore tends
to insulate the fuel pellet from the cladding. When rapid changes in
reactor power are demanded there is a time delay (thermal lag time)
in conducting heat from the pellets to the clad and thus to the cooling
water. This time delay causes a further delay, in addition to the loop
flow time, in transfer of heat from the reactor to the boilers.

The thermal resistance of the gap also causes an increase in
fuel pellet temperature following an increase in reactor heat output.
This sharp rise in fuel temperature causes negative addition of reactivity
into the core through the negative fuel temperature coefficient of reactivity.
The negative reactivity opposes the positive reactivity added by rod
motion. The control system must therefore move the control rods to
override the negative reactivity from the fuel temperature increase.
The thermal conductance of the gap is partly dependent upon the thermal
conductivity of the gas occupying the gap. When the reactor core is new
the gap is filled with helium gas. The thermal conductance of the gap
when filled with helium is fairly good and therefore the thermal lag time
and fuel temperature reactivity effects are moderate. As the core under-
goes irradiation the thermal conductance of the gap becomes lower
because low thermal conductivity fission product gases such as xenon
and kryton mix with the helium. After the first 50 days of operation it
is assumed that the thermal lag time and fuel temperature reactivity
effects are more pronounced causing slower core response.

The control system is provided with adjustments for the
constants K_1 and K_2 of Equations 1 and 2 to compensate for the changing
heat transfer characteristics.

IV. PLANT SIMULATION STUDIES

A. DESCRIPTION

The dynamic analysis of the CETR plant was carried out by first establishing mathematical models describing the thermodynamic and fluid dynamic characteristics of the primary loop components, including reactor core, primary piping, boilers, rod mechanisms and control system, and primary fluid and metal masses. A large number of differential equations result. Solution of these equations is difficult by any means except computers. The analog computer was chosen to obtain the transient solutions required, for the following reasons:

1. Computation is carried out as desired in real time or accelerated time.
2. A record of any variable in the system can be obtained as a continuous function of time.
3. Non-linear operations may be performed continuously.

An extensive analog study was made of the CETR plant to (1) determine the natural response of the plant to normal load transients, (2) investigate various reactor control systems, and (3) make a parametric study of the control system selected. Additional studies were made to determine the relationship of system parameters to control system requirements. Complete details of the simulation models used are given in Appendix B.

B. REPRESENTATIVE PLANT PERFORMANCE CURVES

Sample data from the analog simulation studies are included in this section. These data have been selected as typical examples of the control system and plant responses to various load demand changes. Certain core characteristics are subject to variation as the core under-goes irradiation. These changes were discussed in Section III. The

plant was simulated using parameters representative of the beginning and the end of core life, and both conditions are discussed and illustrated in this section.

The core parameters influencing the control system settings as the core ages are the fuel rod gap conductance and the two temperature coefficients of reactivity. The variation of these parameters from beginning to end of core life, and typical settings of the control system constants, K_1, K_2 and τ are presented in Table II.

TABLE II
CORE PARAMETERS AND CONTROL SYSTEM CONSTANTS SETTINGS

	Beginning of Core Life	End of Core Life
Moderator Temperature Coefficient of Reactivity, $\Delta k/F$	-1.4×10^{-4}	-0.8×10^{-4}
Fuel Temperature Coefficient of Reactivity, $\Delta k/F$	-1×10^{-5}	-1×10^{-5}
Fuel Rod Gap Conductance, Btu/sec-ft^2-F	0.2	0.1175
K_1, sec/lb	13.9×10^{-4} (.85)	13.9×10^{-4} (.85)
K_2, in.^{2}/lb	15×10^{-4} to 22.8×10^{-4}	15×10^{-4} to 22.8×10^{-4}
τ, sec	200	100 and 200

A complete listing of plant parametric data is included in Appendix A. Results of typical response curves are tabulated in Table III for the beginning of core life, and Table IV for the end of core life. With the control system constants set at the values listed in Table II the plant meets the response requirements set forth in Section IV. The data tabulated in Tables III and IV are illustrated graphically on Figures 6 - 14.

C. CONTROL CONSTANTS STUDIES

The effects of varying the control system constants were determined in arriving at the settings prescribed in Table II. These effects are discussed in this section.

As the constant K_1 is brought closer to unity the effect is slightly more power overshoot and a shorter time period for the reactor to reach the new demanded level and subsequently stablize.

The constant K_2 is varied over the core life because of its greater influence on power overshoot. The higher values of K_2 reduce the time required to return steam pressure to normal but cause increased power overshoot. At the beginning of core life heat transfer characteristics are good and core response to power demand changes require less correction from the K_2 term. Excessive power overshoot is possible if K_2 is set too high either early or late in core life. This effect is illustrated on Figure 15. Figure 16 shows that the maximum steam pressure variation is insensitive to the K_2 setting.

The various groups of movable control rods will not have the same worth in terms of reactivity. The range of rod group worth lies between 0.02 $\Delta k/k$ and 0.04 $\Delta k/k$. The lower worth rod groups add less reactivity per unit length of travel than the stronger ones. Therefore, for a demand power change calling for a specified reactivity addition rate, the lower worth rod groups must move at a faster speed than the stronger ones. This effect is accounted for in the CETR control system through the use of variable speed control rod drives. The rod drives are continuously variable from 3 to 22 1/2 inches/minute. A combination of the lowest worth rod group and the power demand needing the greatest reactivity addition rate will not require the drives to exceed the maximum speed. The power demand changes combined with 2% $\Delta k/k$ rod groups are the most difficult for the control system to meet. Most of the studies have used 2% $\Delta k/k$ groups.

TABLE III
TYPICAL PLANT RESPONSES AT BEGINNING OF CORE LIFE

Power Demand	Initial Power, % of Full Power	Final Power, % of Full Power	Overshoot or Undershoot, % of Full Power	Minimum Reactor Period, sec	Steam Pressure Variation, psi	Reference
+ 18.2% Step*	80	98.2	7	89	- 36	Fig. 6
- 18.2% Step	75	56.8	9.8	78	+58	Fig. 7
+ 9.1% per minute** Ramp	20	97.5	6	240	-21	Fig. 8
- 9.1% per minute Ramp	100	20	4	265	+50	Fig. 9

* A step change of 18.2% is equivalent to 106.4 MWt reactor power, or 50 MWe generator demand.

** A ramp change of 9.1% per minute is equivalent to 53.2 MWt per minute reactor power, or 25 MWe per minute generator demand.

- 20 -

TABLE IV

TYPICAL PLANT RESPONSES AT END OF CORE LIFE

Power Demand	Initial Power, % of Full Power	Final Power, % of Full Power	Overshoot or Undershoot, % of Full Power	Minimum Reactor Period, sec	Steam Pressure Variation, psi	Reference
+ 18. 2% Step*	80	98. 2	6	87	-40. 5	Fig. 10
+ 18. 2% Step	80	98. 2	9. 8	67	-41	Fig. 11
- 18. 2% Step	80	61. 8	8. 8	199	+43. 6	Fig. 12
+ 9. 1% per minute** Ramp	20	97. 5	6. 5	265	-47	Fig. 13
- 9. 1% per minute	100	20	5	280	+53	Fig. 14

*   See note Table III.
** See note Table III.

V. CONCLUSIONS

The control system provides a safe and reliable means to control the plant in accordance with the design criteria set forth in Section III of this report. The control system and components have been designed to provide enough flexibility to allow for variations in reactor characteristics during its lifetime. Analog simulation studies verify that intended design requirements have been met.

VI. APPENDICES

APPENDIX A
PLANT PARAMETERS

	Beginning of Life*	End of Life
I. REACTOR KINETICS		
1. Neutron lifetime, sec		2.3×10^{-5}
2. Total delayed neutron fraction		0.00755
3. Decay constant for delayed precursors, sec^{-1}		0.0814
4. Differential rod worth, in.$^{-1}$		variable
5. Moderator temperature coefficient, $\Delta k/F$	-1.4×10^{-4}	-0.8×10^{-4}
6. Fuel Temperature Coefficient of Reactivity, $\Delta k/F$	-1×10^{-5}	-1×10^{-5}
II. AVERAGE FUEL ROD		
1. Fuel density, lb/ft^3		581
2. Specific heat of fuel (C_f), Btu/lb-F		0.057
3. Thermal conductivity of fuel (K_f), Btu/sec-ft-F	0.001181 (818 F)	0.000833 (1257 F)
4. Volume of fuel in core (V_f), ft^3		72.6
5. Radius of fuel pellet (r_f), ft		0.01083
6. Gap conductance (h_g), Btu/sec-ft^2-F	.312	.0782
7. Clad inner radius (r_{ci}), ft		0.01096
8. Specific heat of clad (C_{cl}), Btu/sec-ft-F		0.120
9. Thermal conductivity clad (K_c), Btu/sec-ft-F		0.003333

* Parameters at the beginning of core life are equal to those at the end of core life except where noted.

10. Clad outer radius (r_{cs}), ft ... 0.01267

11. Clad density (clad), lb/ft^3 ... 507

12. Full coolant mass flow rate (w_{co}), lb/sec ... 14,700

13. Film conductance at full flow rate (h_{fo}), $Btu/sec-ft^2-F$ ... 2.53

14. 100% reactor power, Btu/sec ... 554,000

III. AVERAGE COOLANT CHANNEL

1. Total weight of coolant in core (M_c), lb ... 6540

2. Specific heat of coolant (C_c), Btu/lb-F ... 1.155

3. Total effective outer clad area (A_{co}), ft^2 ... 15,600

4. Film conductance at full flow (h_f), $Btu/sec-ft^2-F$ ... 2.53

IV. PIPE SIMULATION

1. Weight of coolant in pipe (M_{pipe})
   (hot leg) $(M_{pipe} \#1)$, lb/loop ... 13,200
   (cold leg) $(M_{pipe} \#2)$, lb/loop ... 18,580

2. Coolant mass (w_c), lb/sec-loop ... 3,680

V. BOILERS

1. Weight of primary coolant in boiler (M_p), lb/boiler ... 17,000

2. Specific heat of primary coolant (C_c), Btu/lb-F ... 1.155

3. Mass flow rate of primary coolant (w_c), lb/sec/boiler ... 3.680

4. Effective boiler heat transfer area (A) ft^2/boiler ... 13,800

5. Weight of secondary (M_s), lb/boiler ... 20,420

6. Steam flow rate (W_s), lb/sec-boiler (full flow) ... 153.4

7. Overall boiler conductance (U), $Btu/sec-ft^2-F$ ... 0.2000

APPENDIX B
PLANT SIMULATION DETAILS

1. REACTOR KINETICS

The standard nuclear kinetic equations used in CETR studies are:

$$\frac{dn}{dt} = \frac{\rho - \beta}{l^*} n + \sum \lambda_i C_i \tag{1}$$

$$\frac{dC_i}{dt} = \frac{\beta_i}{l^*} n - \lambda_i C_i \tag{2}$$

where,

n = normalized neutron density

t = time, sec

ρ = $\dfrac{k_{eff} - 1}{k_{eff}}$ = reactivity

l^* = neutron lifetime, sec

β = $\sum_i \beta_i$ = total delayed neutron fraction

λ_i = decay constant for i^{th} group of delayed neutron precursors, sec^{-1}

C_i = normalized density of precursors in the ith group

β_i = fraction of delayed neutrons in the ith group

In equations (1) and (2), the following assumptions are made: (1) there is a uniform flux distribution, (2) the neutrons are monoenergetic, and (3) integration over space is performed, i.e., spatial variations in neutron density are neglected.

Although the variables in equations (1) and (2) are defined in terms of neutron concentrations, no appreciable error is introduced by assuming that reactor power is directly proportional to neutron concentration. The

The equations may then be restated with "n" redefined as the power production in Btu/sec and "C_i" as the potential power stored in delayed neutrons.

The reactivity, ρ, is computed by the equation

$$\frac{d\rho}{dt} = \frac{\partial\rho}{\partial x}\frac{dx}{dt} + \frac{\partial\rho}{\partial \overline{T}_c}\frac{d\overline{T}_c}{dt} + \frac{\partial\rho}{\partial \overline{T}_f}\frac{d\overline{T}_f}{dt} \tag{3}$$

where,

t = time, sec

x = control rod displacement, in.

$\frac{\partial\rho}{\partial x}$ = control rod worth, in.$^{-1}$

$\overline{T}_c$ = average moderator temperature, F

$\frac{\partial\rho}{\partial \overline{T}_c}$ = moderator temperature coefficient of reactivity, $\Delta k/F$

$\overline{T}_f$ = average fuel temperature, F

$\frac{\partial\rho}{\partial \overline{T}_f}$ = fuel temperature coefficient of reactivity, $\Delta k/F$

It is assumed that reactivity changes due to variations in fuel temperature are treated in the same manner as reactivity changes due to variations in moderator temperature. Moderator and fuel temperature coefficients are computed and used in equation (3).

For simulation of the nuclear kinetics, equation (4) is added.

$$N = n + n_d \tag{4}$$

where

N = normalized reactor power level ($N = 1$ at 100% of full reactor power)

n_d = normalized decay heat

n = normalized neutron density

Computations indicate the response of a kinetic model with six delayed neutron groups is not significantly different from those of a model with one equivalent group. Therefore, equations (1) and (2), which used a six-group model, are replaced by equations (5) and (6), using a one-group model.

$$\frac{dn}{dt} = \frac{\rho - \beta}{l*} \, n + \lambda C \tag{5}$$

$$\frac{dC}{dt} = \frac{\beta}{l*} \, n - \lambda C \tag{6}$$

where β and λ are defined as

$$\beta \equiv \sum_i \beta_i \tag{7}$$

$$\lambda \equiv \sum_i \beta_i \Big/ \sum \frac{\beta_i}{\lambda_i} \tag{8}$$

The computer arrangement for generating the term ΔN, the change in power level, is shown schematically in Fig. 17. Amplifiers 1 and 2, in conjunction with the function generator (F.G.) and the multiplying potentiometers, simulate the effect of the control rods. Calculated differential rod worth curves are reproduced by the function generator. These curves (of the form shown in Fig. 18) are derivatives of the 0.02 Δk and 0.04·Δk curves in Fig. 19 The fuel temperature coefficient effect is introduced by means of amplifier 3 and coefficient potentiometer b. The effect of the moderator temperature is inserted through coefficient potentiometer c. Amplifier 4 sums the three reactivity terms and generates the term ρ, or

$$\Delta \rho = \frac{\partial \rho}{\partial x} \, \Delta x + \frac{\partial \rho}{\partial \overline{T}_c} \, \Delta \overline{T}_c + \frac{\partial \rho}{\partial \overline{T}_f} \, \Delta \overline{T}_f \tag{9}$$

which is a restatement of equation (3).

Parameters used for reactor kinetics are:

$l* = 2.3 \times 10^{-5}$ sec

$\beta = 0.00755$

$\lambda = 0.0814$ sec^{-1}

$\frac{\partial \rho}{\partial x} =$ See Fig. 18

$\frac{\partial \rho}{\partial \overline{T}_c} =$ See Fig. 20 and Appendix A

$\frac{\partial \rho}{\partial \overline{T}_f} = -1 \times 10^{-5}$ $\Delta k/F$ (See Fig. 21)

Equations (5), (6), and (9) are simulated by the following computer equations.

$$\dot{n} = 13.04 \, [10^5 \, pn/30] - [\dot{\Delta C}] \tag{10}$$

$$\frac{\dot{\Delta C}}{2} = 3.283 \, [50 \, \Delta n] - 0.0814 \, [\Delta C/2] \tag{11}$$

$$10^5 \, p/15 = 3.333 \, [10^4/5 \, \frac{\partial p}{\partial x} \, x] - (0.533) \, [T_c] \qquad \text{(See Note)}$$

$$- 0.5333 \, [\Delta T_f/8] \tag{12}$$

2. THERMAL MODEL OF REACTOR

The thermal model of the core is assumed to consist of an "average" fuel rod and its associated "average" coolant channel. Other assumptions pertaining to this model are:

1. The densities, specific heats, thermal conductivities, and dimensions of fuel and clad materials are constant.
2. Only radial heat conduction is considered. (Axial and peripheral components of conduction are neglected.)
3. Volumetric heat generation within the fuel is independent of position in the fuel.
4. Heat storage in the helium gap is negligible.
5. Flow in the average coolant channel is turbulent.
6. Heat storage in the supporting structure is negligible.

a. Average Fuel Rod

The equations describing the average fuel rod are

$$\rho_f \, C_f \, \frac{\partial T_f}{\partial t} = K_f \left[\frac{\partial^2 T_f}{\partial r^2} + \frac{1}{r} \, \frac{\partial T_f}{\partial r} \right] + \frac{aN}{V_f} \; ; \quad 0 \le r \le r_f \tag{13}$$

with the boundary conditions

$$\left(\frac{\partial T_f}{\partial r} \right)_{r=0} = 0 \tag{14}$$

and

Note: Top numbers are beginning of core life constants
Numbers in parenthesis are end of core life constants

$$-K_f A_{fs} \left(\frac{\partial T_f}{\partial r} \right)_{r=r_f} = h_{gap} A_{ci} \left[T_f (r_f, t) - T_{clad} (r_{ci}, t) \right] \qquad (15)$$

$$\bar{T}_f = \frac{1}{\pi r_f^2} \int_0^{2\pi} \int_0^{r_f} T_f (r, t) \, r \, dr \, d\theta = \frac{2}{r_f^2} \int_0^{r_f} T_f (r, t) \, r dr \qquad (16)$$

$$\rho_{clad} C_{clad} \frac{\partial T_{clad}}{\partial t} = K_{clad} \left[\frac{\partial^2 T_{clad}}{\partial r^2} + \frac{1}{r} \frac{\partial T_{clad}}{\partial r} \right]^0 ; \ r_{ci} \leq r \leq r_{co} \quad (17)$$

with the boundary conditions

$$h_{gap} A_{co} \left[T_f (r_f, t) - T_{clad} (r_{ci}, t) \right] = -K_{clad} A_{ci} \left[\frac{\partial T_{clad}}{\partial r} \right]_{r=r_{ci}} \qquad (18)$$

and

$$-K_{clad} A_{co} \left[\frac{\partial T_{clad}}{\partial r} \right]_{r=r_{co}} = h_f A_{co} \left[T_{clad} (r_{co}, t) - \bar{T}_c (t) \right] \qquad (19)$$

$$h_f = h_{fo} \left(\frac{W_c}{W_{co}} \right)^{0.8} \qquad (20)$$

where

ρ_f = fuel density, lb/ft^3

C_f = specific heat of fuel, Btu/lb-F

$T_f(r, t)$ = fuel temperature, F

t = time, sec

K_f = thermal conductivity of fuel, Btu/sec-ft^2-F/ft

r = radial distance, ft

$N(t)$ = normalized ($N = 1$ at full power) reactor power level

α = 100% reactor power, Btu/sec

V_f = total volume of fuel in core, ft^3

r_f = radius of fuel pellet, ft

A_{fs} = total fuel surface area, ft^2

A_{co} = total outer clad surface area, ft^2

A_{ci} = total inner clad surface area, ft^2

h_{gap} = conductance, referred to outer clad radius, Btu/sec-ft^2-F

$T_{clad}(r, t)$ = clad temperature, F

r_{ci} = inner radius of clad, ft

$\overline{T}_f(t) =$ average fuel temperature, F

$\rho_{clad} =$ clad density, lb/ft^3

$C_{clad} =$ specific heat of clad, Btu/lb-F

$K_{clad} =$ thermal conductivity of clad, $Btu/sec-ft^2-F/ft$

$r_{co} =$ outer radius of clad, ft

$\overline{T}_c(t) =$ average temperature of water in average coolant channel, F

$h_f =$ film conductance referred to outer clad radius, $Btu/sec-ft^2-F$

$W_c =$ coolant mass flow rate, lb/sec

$W_{co} =$ full coolant mass flow rate, lb/sec

$h_{fo} =$ film conductance at full flow, $Btu/sec-ft^2-F$

By simulating thermal systems on an incremental basis rather than on total quantity, the need for considering initial conditions is eliminated when dealing with linear systems. For non-linear systems, initial conditions are conveniently inserted. In either event, the difficulty of exactly balancing initial conditions on the computer is eliminated. For example, define

$$T_f(r, t) \equiv T_f(r, 0^-) + \Delta T_f(r, t) \tag{21}$$

$$N(t) \equiv N(0^-) + \Delta N(t) \tag{22}$$

$$T_{clad}(r, t) \equiv T_{clad}(r, 0^-) + \Delta T_{clad}(r, t) \tag{23}$$

$N(t)$ is related to $n(t) = n + n_d$, where n_d represents power due to decay heat. This factor is assumed constant in most of the studies ($\Delta N = \Delta n$).

Substituting equations (21) and (22) into equation (13), the following is obtained:

$$\rho_f C_f \frac{\partial}{\partial t} \Delta T_f = K_f \frac{\partial^2}{\partial r^2} T_f(r, 0^-) + \frac{1}{r} K_f \frac{\partial}{\partial r} T_f(r, 0^-)$$

$$+ K_f \frac{\partial^2}{\partial r^2} \Delta T_f(r, t) + \frac{1}{r} K_f \frac{\partial}{\partial r} \Delta T_f(r, t) + \frac{a}{V_f} N(0^-) + \frac{a}{V_f} \Delta N(t) \tag{24}$$

where time $t = 0^*$ corresponds to a steady-state condition.

- 34 -

At t = 0, the system is subject to disturbances, i.e., the computer is placed in the "operate" condition. At this point, the sum of the first, second, and fifth terms on the right-hand side of equation (24) is zero and

$$\rho_f C_f \frac{\partial}{\partial t} \Delta T_f = K_f \left[\frac{\partial^2}{\partial r^2} \Delta T_f + \frac{1}{r} \frac{\partial}{\partial r} \Delta T_f \right] + \frac{a}{V_f} \Delta N \qquad (25)$$

Equations (14) and (15), governing boundary conditions, become

$$\left[\frac{\partial}{\partial r} \Delta T_f \right]_{r=0} = 0 \qquad (26)$$

and

$$-K_f A_{fs} \left(\frac{\partial}{\partial r} \Delta T_f \right)_{r=r_f} = h_{gap} A_{co} [\Delta T_f(r_f, t) - \Delta T_{clad}(r_{ci}, t)] \qquad (27)$$

Analog solution of these equations is best approached by approximating all space derivatives by finite-differences, i.e., the interval $(0, r_f)$ is divided in J equal sub-intervals. To simplify notation,

$$F = -K_f \frac{\partial}{\partial r} \Delta T_f \qquad (28)$$

and

$$\theta = \Delta T_f \qquad (29)$$

The quantities θ and F are evaluated at the points shown in Fig. 22. Each sub-interval is of length $\Delta = \frac{r_f}{J}$. With approximations

$$F_j = -K_f \frac{\theta_{j+1/2} - \theta_{j-1/2}}{\Delta}; \quad j = 1, - - - -, J-1; \qquad (30)$$

and

$$F_{j+1/2} = \frac{F_j + F_{j+1}}{2}; \quad j = 0, - - - -, J-1; \qquad (31)$$

the system of equations to be solved by the computer becomes:

$$F_0 = -K_f \frac{\theta_{1/2} - \theta_0}{\Delta/2} = 0 \qquad (32)$$

$$F_J = -K_f \frac{\theta_J - \theta_{J-1/2}}{\Delta/2} = h_{gap} \frac{A_{ci}}{A_{fs}} [\theta_J - \Delta T_{ci}] \qquad (33)$$

- 35 -

$$\theta_{j+1/2} = \frac{a\Delta N}{M_f C_f} - \frac{1}{\rho_f C_f \Delta} \left[(F_{j+1} - F_j) + \frac{1}{2j+1} (F_j + F_{j+1}) \right] ;$$

$$j = 0, - - -, J-1 \qquad (34)$$

It is observed that if one of the two unknowns (θ or F) could be eliminated from these equations, the computer setup would require fewer amplifiers and more potentiometers.

The problem of determining the minimum allowable J can be approached by any of the following methods:

1. Compare transfer functions for successive values of J if the system is linear.

2. Solve the original system analytically for a representative disturbance, then comparison of response with computer responses for successive values of J.

3. Compare computer responses for successive values of J for a given disturbance.

Method 3 is chosen because it provides a good check on the result and requires less time to execute. A value of J = 5 proved quite satisfactory for the CETR studies.

Similar approximations applied to the clad are represented by equations (17), (18), and (19). Temperatures computed at the clad surfaces and halfway between surfaces are shown in Fig. 23.

The finite-difference approximations yield

$$h_{gap} \frac{A_{co}}{A_{ci}} (\theta_J - \Delta T_{ci}) = \frac{-K_{clad}}{\dfrac{r_{co}-r_{ci}}{2}} (\Delta \overline{T}_{clad} - \Delta T_{ci}), \qquad (35)$$

$$\frac{-K_{clad}}{\dfrac{r_{co}-r_{ci}}{2}} (\Delta T_{co} - \Delta \overline{T}_{clad}) = h_f (\Delta T_{co} - \Delta \overline{T}_c) \qquad (36)$$

$$\Delta \dot{\overline{T}}_{clad} = \frac{2K_{clad}}{\rho_{clad} C_{clad} (r_{co}-r_{ci})} \left\{ \frac{1}{r_{co}-r_{ci}} \left[(\Delta T_{co} - \Delta \overline{T}_{clad}) - \right. \right.$$

$$\left. \left. (\Delta \overline{T}_{clad} - \Delta T_{ci}) \right] + \frac{1}{r_{co} r_{ci}} (\Delta T_{co} - \Delta T_{ci}) \right\} \qquad (37)$$

- 36 -

To compute $\Delta \overline{T}_f$, equations (16) and (21) give

$$\Delta \overline{T}_f = \frac{1}{\pi r_f^2} \int_0^{2\pi} d\theta \cdot \int_0^{r_f} \Delta T_f \, r dr = \frac{2}{r_f^2} \int_0^{r_f} \Delta T_f \, r dr = \frac{2}{r_f^2} \left[\int_0^{r_f/J} \Delta T_f \, r dr + \right.$$

$$\int_{r_f/J}^{2r_f/J} \Delta T_f \, r dr + - - - - + \int_{jr_f/J}^{(j+1)r_f/J} \Delta T_f \, r dr + - - - - + \tag{38}$$

$$\left. \int_{(J-1)r_f/J}^{r_f} \Delta T_f \, r dr \right]$$

By definition,

$$\theta_{j+1/2} \int_{jr_f/J}^{(j+1)r_f/J} r dr = \int_{jr_f/J}^{(j+1)r_f/J} \Delta T_f \, r dr; \quad j=0, - - - - -, J-1 \tag{39}$$

Equation (34) then becomes

$$\Delta \overline{T}_f = \frac{1}{J^2} \, \theta_{1/2} + \frac{3}{J^2} \, \theta_{3/2} + - - - - + \frac{2j+1}{J^2} \theta_{j+1/2} + - - - - +$$

$$\frac{2J-1}{J^2} \, \theta_{J-1/2} \tag{40}$$

For constant flow, equation (20) is not considered in the computer setup. Since the film conductance, h_f, is constant throughout a run, and the only need for (20) is to calculate the constant h_f, if $W_c \neq W_{co}$.

The computer setup for solution of equations (32), (33), (34), (30), (35), (36), (37), and (40), for $J = 5$, is shown in Fig. 24 and Fig. 25. The appropriate computer equations are:

$$\dot{T}_{1/2 \ 20} = 0.2304 \, [50 \Delta N] - \frac{3.040}{(2.144)} \left[\frac{T_{1/2} - T_{3/2}}{4} \right] \tag{41}$$

<div align="right">(See Note Pg. 32)</div>

$$\dot{T}_{3/2}\Big/20 = 0.2304\,[50\Delta N] + \begin{matrix}1.013\\(0.7146)\end{matrix}\left[\frac{T_{1/2}-T_{3/2}}{4}\right] \quad\text{(See Note Pg. 32)}$$

$$\begin{matrix}2.027\\(1.429)\end{matrix}\left[\frac{T_{3/2}-T_{5/2}}{4}\right] \qquad (42)$$

$$\dot{T}_{5/2}\Big/20 = 0.2304\,[50\Delta N] + \begin{matrix}1.216\\(0.8575)\end{matrix}\left[\frac{T_{3/2}-T_{5/2}}{4}\right] -$$

$$\begin{matrix}1.824\\(1.286)\end{matrix}\left[\frac{T_{5/2}-T_{7/2}}{4}\right] \qquad (43)$$

$$\dot{T}_{7/2}\Big/20 = 0.2304\,[50\Delta N] + \begin{matrix}1.303\\(0.9188)\end{matrix}\left[\frac{T_{5/2}-T_{7/2}}{4}\right] -$$

$$\begin{matrix}1.737\\(1.225)\end{matrix}\left[\frac{T_{7/2}-T_{9/2}}{4}\right] \qquad (44)$$

$$\dot{T}_{9/2}\Big/20 = 0.2304\,[50\Delta N] + \begin{matrix}1.351\\(0.9528)\end{matrix}\left[\frac{T_{7/2}-T_{9/2}}{4}\right]$$

$$\begin{matrix}3.378\\(2.382)\end{matrix}\left[\frac{T_{9/2}-T_{5/2}}{4}\right] \qquad (45)$$

$$\overline{T}_{f/8} = 1/2\left\{0.2\left[\frac{T_{1/2}}{20}\right] + 0.6\left[\frac{T_{3/2}}{20}\right] + \left[\frac{T_{5/2}}{20}\right] + 1.4\left[\frac{T_{7/2}}{20}\right] + \right.$$

$$\left.1.8\left[\frac{T_{9/2}}{20}\right]\right\} \qquad (46)$$

$$T_{5/8} = 1/4\left\{\begin{matrix}7.656\\(9.068)\end{matrix}\left[\frac{T_{9/2}}{20}\right] + \begin{matrix}0.22456\\(0.09328)\end{matrix}\left[\frac{T_{ci}}{2}\right]\right\} \qquad (47)$$

$$\frac{T_{ci}}{2} = \begin{matrix}9.270\\(9.773)\end{matrix}\left[\frac{\overline{T}_{clad}}{20}\right] + \begin{matrix}0.3434\\(0.09074)\end{matrix}\left[\frac{T_{5/2}}{8}\right] \qquad (48)$$

42

- 38 -

$$\frac{\overline{T}_{clad}}{20} = \frac{4.015}{(4.015)} \left[\frac{T_{co} - T_{clad}}{2}\right] + \frac{2.222}{(1.567)} \left[\frac{T_{9/2} - T_{5/2}}{4}\right] \tag{49}$$

$$\frac{T_{co}}{2} = \frac{\overline{T}_c}{2} - 2.051 \left[\frac{T_{co} - \overline{T}_{clad}}{2}\right] \tag{50}$$

The parameters used for the average fuel rod simulation are listed in Appendix A, Section II, Average Fuel Rod.

b. Average Coolant Channel

The average coolant channel associated with the Average Fuel Rod of the thermal model is represented by the equations:

$$M_c C_c \frac{\partial T_c}{\partial t} + W_c L_c C_c \frac{\partial T_c}{\partial x} = h_f A_{co} \left[T_{clad}(r_{co}, x, t) - T_c(x, t)\right] \tag{51}$$

$$\overline{T}_c(t) = \frac{1}{L_c} \int_0^{L_c} T_c(x, t)\,dx \tag{52}$$

where

M_c = total weight of coolant in core, lb

C_c = specific heat of coolant, Btu/lb-F

$T_c(x, t)$ = coolant temperature, F

t = time, sec

x = distance in direction of coolant flow, ft

W_c = coolant mass flow, lb/sec

L_c = total effective core length, ft

h_f = film conductance, Btu/sec-ft^2-F

A_{co} = total effective outer clad surface area, ft^2

$T_{clad}(r_{co}, x, t)$ = temperature of outer clad surface, F

$\overline{T}_c(t)$ = average temperature of coolant in core, F

In equations (51) and (52) it is assumed that:

1. Flow in the average coolant channel is turbulent.
2. There is no boiling in the average channel.
3. Heat storage in supporting structure is negligible.
4. The coolant is incompressible.

To simplify notation, $T_{clad}(r_{co}, x, t) = T_{co}(x, t)$. Since flow is constant and all occurrences of "T" in the equation may be replaced by "T", then equations (51) and (52) become:

$$M_c C_c \frac{\partial}{\partial t} \Delta T_c + W_c L_c C_c \frac{\partial}{\partial x} \Delta T_c = h_f A_{co} [\Delta T_{co} - \Delta T_c] \tag{53}$$

$$\Delta \bar{T}_c(t) = \frac{1}{L_c} \int_0^{L_c} \Delta T_c(x, t)\, dx \tag{54}$$

From this point, the approach to the simulation problem depends primarily on two factors: (1) the amount of equipment available, and (2) the parameters of the primary loop. The core transit time is a small fraction of the total loop time. Model studies show that for constant flow, equations (53) and (54) may be replaced by equations:

$$\Delta \dot{T}'_{ri} + \frac{2W_c}{M_c} \Delta T'_{ri} = \frac{2W_c}{M_c} \Delta T_{ri} \tag{55}$$

$$M_c C_c \Delta \dot{\bar{T}}_c + W_c C_c (\Delta T'_{ro} - \Delta T'_{ri}) = h_f A_{co} (\Delta T_{co} - \Delta \bar{T}_c) \tag{56}$$

$$\Delta \dot{T}_{ro} + \frac{2W_c}{M_c} \Delta T_{ro} = \frac{2W_c}{M_c} \Delta T'_{co} \tag{57}$$

$$\Delta \bar{T}_c = 1/2 (\Delta T'_{ri} + \Delta T'_{ro}) \tag{58}$$

where

$$\Delta T_{ri}(t) \equiv \Delta T_c(0, t) \tag{59}$$

$$\Delta T_{ro}(t) \equiv \Delta T_c(L_c, t) \tag{60}$$

In this model it is assumed that the coolant enters the core at temperature T_{ri}, is delayed (the delay being approximated by a first-order lag) by half the core transit time, and arrives at the center of the

core at temperature T'_{ri}. All heat transfer from fuel rod to coolant is assumed to occur at the center of the core, causing the fluid temperature to suddenly increase to T'_{ro}. Then the coolant is delayed (again approximated by a first-order leg) by half the core transit time, and emerged from the core at temperature T_{ro}.

In this model, single slab radial diffusion is assumed. The core inlet water temperature is delayed by a time equal to one-half the core pass time for the outlet temperature.

The equations

$$M_c C_c \frac{\partial T_c}{\partial t} + W_c L_c C_c \frac{\partial T_c}{\partial x} = h_f A_{co} [T_{clad}(r_{co}, t) - T_c(x, t)] \tag{61}$$

and

$$T_c(t) = \frac{1}{L_c} \int_0^{L_c} T_c(x, t) dx \tag{62}$$

are simulated in the analog by the circuit shown in Fig. 26.

The computer equations describing the average coolant channel are:

$$\overline{\dot{T}}_c/10 = \underset{(0.3925)}{0.3925} [T_{co} - \overline{T}_c] - \underset{(0.450)}{0.450} [\overline{T}_c - T'_{ri}] \qquad \text{(See Note Pg. 32)} \tag{63}$$

$$T'_{ro} = 2\overline{T}_c - T'_{ri} \tag{64}$$

$$\dot{T}'_{ri} = \underset{(4.50)}{4.50} [T_{ri} - T'_{ri}] \tag{65}$$

$$\dot{T}_{ro} = \underset{(4.50)}{4.50} [T'_{ro} - T_{ro}] \tag{66}$$

$$\frac{T_p(0)}{T_{ro}} = \frac{p^2 - 1.6728 p + 0.9328}{p^2 + 1.6728 p + 0.9328} \cdot \frac{1}{1+p} \tag{67}$$

$$\frac{T_{ri}}{T_p(L)} = \frac{p^2 - 1.1884 p + 0.4708}{p^2 + 1.1884 p + 0.4708} \cdot \frac{1}{1+p} \tag{68}$$

The parameters used in the Average Coolant Channel Simulation are tested in Appendix A, Section III.

- 41 -

c. **Pipes**

For the pipes connecting reactor and boilers, the following assumptions are made:

1. The pipes are perfectly insulated.
2. Heat storage in the pipe walls is negligible.
3. Flow in the pipes is turbulent.
4. The coolant is incompressible.

Therefore the equations describing the pipes become

$$M_{pipe} C_c \frac{\partial T_{pipe}}{\partial t} + W_c L_{pipe} C_c \frac{\partial T_{pipe}}{\partial x} = 0 \qquad (69)$$

$$\bar{T}_{pipe} = \frac{1}{L_{pipe}} \int_0^{L_{pipe}} T_{pipe} (x, t) dx \qquad (70)$$

where:

M_{pipe} = weight of coolant in pipe, lb
C_c = specific heat of coolant, Btu/lb-F
$T_{pipe}(x, t)$ = temperature of coolant in pipe, F
t = time, sec
W_c = coolant mass flow rate, lb/sec
L_{pipe} = length of pipe, ft
x = distance in direction of coolant flow, ft
$\bar{T}(t)_{pipe}$ = average temperature of coolant in pipe, F

Since

$$M_{pipe} = \rho_c A_{pipe} L_{pipe} \qquad (71)$$

and

$$W_c = \rho_c A_{pipe} V_c \qquad (72)$$

where

ρ_c = density of coolant, lb/ft^3
A_{pipe} = cross-sectional area of pipe, ft^2
V_c = velocity of coolant flow, fps

Equation (69) then is written

$$\frac{\partial T_{pipe}}{\partial t} + V_c \frac{\partial T_{pipe}}{\partial x} = 0 \qquad (73)$$

- 42 -

Equation (73) implies that

$$\mathcal{J}_{pipe}(L_{pipe}, t) = \mathcal{J}_{pipe}\left(0, t - \left(\frac{L_{pipe}}{V_c}\right)\right) \tag{74}$$

if V_c is constant; or, in terms of Laplace transforms

$$\mathcal{J}_{pipe}(L_{pipe}, S) = \mathcal{J}_{pipe}(0, s)e^{-\frac{L_{pipe}}{V_c}s} \tag{75}$$

where

$$\mathcal{J}_{pipe}(x, s) = \mathcal{L}\left\{\mathcal{J}_{pipe}(x, t)\right\} \tag{76}$$

Therefore, with regard to coolant temperatures, the pipe represents a pure time delay of

$$\tau = \frac{L_{pipe}}{V_c} \text{ sec} \tag{77}$$

(It should be noted that the above equations apply for ΔTs as well as total Ts since $\frac{\partial}{\partial x} T_p(x, 0^-) = 0$.

Standard electronic analog computer components were regarded as adequate to approximate pure delays and the use of direct analogs of transport delay, such as magnetic tape equipment or curve followers, were not deemed necessary.

Several approaches to the problem of time-delay simulation have been made on the basis of approximating the transfer function $e^{-\tau s}$. The circuit which has been used for the CETR studies is taken from the article by W. J. Cunningham, "Time-Delay Networks for an Analog Computer", published in I R.E. Transactions, December, 1955. Cunningham's approach is based on the fact that for the transfer function $e^{-\tau s}$, with $e^{-\tau s}$ replaced by jw, the phase plot is linear while the amplitude ratio is unity. He derives 2-, 4-, 6-, and 8-root networks and an index of accuracy (figure of merit) for each. The 4-root network, shown in Fig. 27, is adequate for the CETR studies.

The potentiometer settings are computed from

$$\frac{M}{W} = \frac{L}{V} = \tau = \frac{3}{a} \tag{78}$$

$$\frac{b}{a} = \frac{\sqrt{3}}{3} \tag{79}$$

where:

M	=	weight of coolant in pipe, lb
W	=	coolant mass flow rate, lb/sec
L	=	total length of pipe, ft
V	=	velocity of coolant flow, ft/sec
τ	=	time delay, sec

d. **Boilers**

For the boilers, it is assumed that

1. Flow in the primary tubes is turbulent.
2. The coolant is incompressible.
3. Heat storage in the tube walls is negligible.
4. Heat storage of the water only is considered on the secondary side.
5. All of the secondary water mass is at one temperature (the steam temperature) at any instant.

The boiler equations consistent with the above assumptions are

$$M_p C_c \frac{\partial T_p}{\partial t} + W_c L_p C_c \frac{\partial T_p}{\partial x} + UA_T (T_p - T_s) = 0 \tag{80}$$

$$C_s \frac{d(M_s T_s)}{dt} = UA_T (\overline{T}_p - T_s) - (W_s h_s - W_{feed} h_{feed}) \tag{81}$$

$$\overline{T}_p (t) = \frac{1}{L_p} \int_0^{L_p} T_p (x, t) \, dx \tag{82}$$

$$\frac{dM_s}{dt} = W_c - W_s \tag{83}$$

where

M_p	=	weight of primary coolant in boiler, lb
C_c	=	specific heat of primary coolant, Btu/lb-F
$T_p(t)$	=	primary coolant temperature, F
t	=	time, sec
W_c	=	mass flow rate of primary coolant, lb/sec
L_p	=	total effective boiler length, ft
x	=	distance in direction of primary coolant flow, ft

- 44 -

U = boiler conductance, Btu/sec-ft^2-F

A_T = total effective boiler heat transfer area, ft^2

$T_s(t)$= secondary water (and steam) temperature, F

C_s = specific heat of secondary water, Btu/lb-F

M_s = weight of secondary, lb

$T_p(t)$= average temperature of primary coolant, F

W_s = steam flow rate, lb/sec

h_s = steam enthalpy, Btu/lb

$W_{feed}(t)$ = feedwater flow rate, lb/sec

h_{feed} = feedwater enthalpy, Btu/lb

For the majority of applications the variation of secondary water mass M_s is negligible. In such cases, equation (83) may be ignored and equation (82) becomes

$$M_s C_s \frac{d T_s}{dt} = UA (T_p - T_s) - P \tag{84}$$

where

$$P(t) = W_s h_s - W_{feed} h_{feed} \tag{85}$$

is the steam power demand in Btu/sec.

For a more general type of heat exchanger (e.g., parallel flow or counter flow) both T_p and T_s are functions of x. The fact that the T_s here is independent of x makes the simulation problem much simpler than otherwise. To simplify notation, let

$$A \equiv \frac{W_c}{M_p} \tag{86}$$

$$B \equiv \frac{UA_T}{M_p C_c} \tag{87}$$

$$C \equiv \frac{UA_T}{M_s C_s} \tag{88}$$

$$D \equiv \frac{1}{M_s C_s} \tag{89}$$

The time varying quantities $T_p(x, t)$, $T_s(t)$, $T_p(t)$, and $P(t)$ may each be broken up into steady-state and transient components. If the steady-state is assumed to hold up to time $t = 0$, then

$$T_p(x, t) = T_p(x, 0^-) + \Delta T_p(x, t) \tag{90}$$

$$T_s(t) = T_s(0^-) + \Delta T_s(t) \tag{91}$$

$$T_p(t) = \overline{T}_p(0^-) + \Delta \overline{T}_p(t) \tag{92}$$

$$P(t) = P(0^-) + \Delta P(t) \tag{93}$$

With these definitions, equations (80), (84), and (82) become, respectively,

$$\frac{\partial \Delta T_p}{\partial t} + AL_p \frac{\partial \Delta T_p}{\partial x} + B\Delta T_p - B\Delta T_s$$
$$+ \left[AL_p \frac{\partial}{\partial x} T_p(x, 0^-) + BT_p(x, 0^-) - BT_s(0^-) \right] \tag{94}$$

$$\frac{\partial \Delta T_s}{\partial t} - C\Delta T_{p_L} + C\Delta T_s + D\Delta P + [-C\overline{T}_p(0^-) + CT_s(0^-) + $$

$$DP(0^-)] = 0 \tag{95}$$

$$\Delta \overline{T}_p = \frac{1}{L_p} \int_0^{L_p} \Delta T_p \, dx + \left[\frac{1}{L_p} \int_0^{L_p} T_p(x, 0^-) \, dx - \overline{T}_p(0^-) \right] \tag{96}$$

The bracketed quantities in equations (94), (95), and (96) are identically zero by definition of steady-state and the boiler equations on an incremental basis are

$$\frac{\partial \Delta T_p}{\partial t} + AL_p \frac{\partial \Delta T_p}{\partial x} + B\Delta T_p - B\Delta T_s = 0 \tag{97}$$

- 46 -

$$\frac{\partial \Delta T_s}{\partial t} - C \Delta \bar{T}_p + C \Delta T_s + D \Delta P = 0 \tag{98}$$

$$\Delta \bar{T}_p = \frac{1}{L_p} \int_0^{L_p} \Delta T_p \, dx \tag{99}$$

in which the _initial_ values of ΔT_p, ΔT_s, ΔT_p, and ΔP are all zero. Here, as before, script letters will be used to denote the Laplace transforms of the corresponding functions of time; i.e.:

$$\mathcal{L}\left\{\Delta T_p (x, t)\right\} = \Delta \mathcal{T}_p (x, s) \tag{100}$$

$$\mathcal{L}\left\{\Delta T_s (t)\right\} = \Delta \mathcal{T}_s (s) \tag{101}$$

$$\mathcal{L}\left\{\Delta \bar{T}_p (t)\right\} = \Delta \mathcal{T}_p (s) \tag{102}$$

$$\mathcal{L}\left\{\Delta P (t)\right\} = \Delta \mathcal{P}(s) \tag{103}$$

The Laplace transforms of (97), (98), and (99) are

$$S \Delta \mathcal{T}_p + A L_p \frac{\partial}{\partial x} \Delta \mathcal{T}_p + B \Delta \mathcal{T}_p - B \Delta \mathcal{T}_s = 0 \tag{104}$$

$$S \Delta \mathcal{T}_s - C A \mathcal{T}_p + C A \mathcal{T}_s + D A \mathcal{P} = 0 \tag{105}$$

$$\Delta \mathcal{T}_p = \frac{1}{L_p} \int_0^{L_p} \Delta \mathcal{T}_p \, dx \tag{106}$$

Equation (104) may be written

$$\frac{\partial \Delta \mathcal{T}_p}{\partial x} (x, s) + \frac{S+B}{A L_p} \Delta \mathcal{T}_p (x, s) = \frac{B}{A L_p} \Delta \mathcal{T}_s (s) \tag{107}$$

and the solutions of (106) are

- 47 -

$$\Delta \mathcal{J}_p(x, s) = e^{-\int_0^x \frac{S+B}{AL_p} dq} \left\{ \Delta \mathcal{J}_p(0, s) + \int_0^x \frac{B}{AL_p} \Delta \mathcal{J}_s(s) \, e^{\int_0^q \frac{S+B}{AL_p} dp} dq \right\}$$

$$= e^{-\frac{S+B}{AL_p} x} \left\{ \Delta \mathcal{J}_p(0, s) + \frac{B}{AL_p} \Delta \mathcal{J}_s(s) \int_0^x e^{\frac{S+B}{AL_p} q} dq \right\}$$

$$= e^{-\frac{S+B}{AL_p} x} \left\{ \Delta \mathcal{J}_p(0, s) + \frac{B}{S+B} \Delta \mathcal{J}_s(s) \left(e^{\frac{S+B}{AL_p} x} - 1 \right) \right\} \qquad (108)$$

or

$$\Delta \mathcal{J}_p(x, s) = \Delta \mathcal{J}_p(0, s) \, e^{-\frac{S+B}{AL_p}} + \frac{B}{S+B} \Delta \mathcal{J}_s(s) \, (1 - e^{-\frac{S+B}{AL_p} x}) \qquad (109)$$

$$\Delta \mathcal{J}_p(L_p, s) = \Delta \mathcal{J}_p(0, s) \, e^{-\frac{S+B}{A}} + \frac{B}{S+B} \Delta \mathcal{J}_s(s) \, (1 - e^{-\frac{S+B}{A}}) \qquad (110)$$

Integration of (104) with regard to x from 0 to L_p and substitution of (106) gives

$$S \Delta \bar{\mathcal{J}}_p + A [\Delta \mathcal{J}_p(L_p, s) - \Delta \mathcal{J}_p(0, s)] + B \Delta \bar{\mathcal{J}}_p - B \Delta \mathcal{J}_s = 0$$

from which

$$\Delta \bar{\mathcal{J}}_p = \frac{A [\Delta \mathcal{J}_p(0, s) - \Delta \mathcal{J}_p(L_p, s)] + B \Delta \mathcal{J}_s}{S+B} \qquad (111)$$

Solving equation (105) for

$$\Delta \mathcal{J}_s = \frac{C \Delta \bar{\mathcal{J}}_p - D \Delta \mathcal{P}}{S+C} \qquad (112)$$

The boiler simulator is required to take as input the quantities $\Delta T_p(0, t)$ (boiler primary inlet temperature) and $\Delta P(t)$ (steam power demand); and to compute and furnish as output the quantities $\Delta T_p(L_p, t)$ (boiler primary outlet temperature), $\Delta T_p(t)$ (average primary coolant temperature), and

- 48 -

$\Delta T_s(t)$ (steam temperature). There are three "unknowns", and three equations (110), (111), and (112) are available for computing these unknowns.

A computer component having the following transfer function is assumed.

$$e^{-\frac{S+B}{A}} = e^{-\frac{S}{A}} \cdot e^{-\frac{B}{A}} \tag{113}$$

and the computer circuit for the solution of these equations is derived. Figure 28a shows the circuit for (110).

Figure 28b shows the circuit for (111).

The circuit for (112) is shown in Fig. 28c.

The complete boiler simulator circuit is obtained by combining the three circuits as shown in Fig. 29.

It should be noted that the computer circuit of Fig. 29 represents an _exact_ solution of equations (110), (111), and (112). The only practical difficulty is the realization of the transfer function $e^{-\frac{S}{A}}$, as shown in Fig. 30. This simulation was tested and found as good as an eight-section boiler simulator based on finite-difference methods.

If the assumption of constant secondary water mass (M_s) is not justified, then equation (81) must be used as written, and (83) must be considered. Moreover, supplementary information is required regarding the manner in which W_{feed} varies with steam power demand. Ideally, this information would be in the form of equations describing the boiler feedwater regulator.

There is one additional difficulty in connection with variable M_s. If the quantities U, h_s, and h_{feed} are constants, then with the definitions (91), (92), and

$$M_s(t) = M_s(0^-) + \Delta M_s(t) \tag{113}$$

$$W_s(t) = W_s(0^-) + \Delta W_s(t) \tag{114}$$

$$W_{feed}(t) = W_{feed}(0^-) + \Delta W_{feed}(t) \tag{115}$$

Equation (81) becomes

$$C_s [M_s(0^-) + \Delta M_s(t)] \frac{d\Delta T_s}{dt} + C_s [T_s(0^-) + \Delta T_s(t)] \frac{d\Delta M_s}{dt}$$

$$= UA_T [\bar{T}_p(0^-) - T_s(0^-)] + UA_T [\Delta \bar{T}_p(t) - \Delta T_s(t)]$$

$$- [W_s(0^-) h_s - W_{feed}(0^-)] - [\Delta W_s(t) h_s - \Delta W_{feed} h_{feed}] \qquad (116)$$

The first and third terms on the right side of equation (109) must cancel, so the equation reduces to

$$C_s [M_s(0^-) + \Delta M_s(t)] \frac{d\Delta T_s}{dt} + C_s [T_s(0^-) + \Delta T_s(t)] \frac{d\Delta M_s}{dt}$$

$$\qquad (117)$$

$$= UA_T [\Delta \bar{T}_p(t) - \Delta T_s(t)] - [\Delta W_s(t) h_s - \Delta W_{feed} h_{feed}]$$

The terms $C_s M_s(0^-) \frac{d\Delta T_s}{dt}$ and $C_s T_s(0^-) \frac{d\Delta M_s}{dt}$, which did not appear for constant M_s, <u>must</u> be accounted for in the simulation. Thus, even for simulation on an incremental basis, some initial conditions must be considered if a differential equation has variable coefficients.

The boiler simulation is shown in Fig. 30 using the following computer equations:

$$T_p(L) = 0.527 \left[e^{-\frac{s}{0.2585}} \right] \left[T_p(0) - \frac{0.1657 T_s}{p + 0.1657} \right] + \frac{0.1657 T_s}{p + 0.1657} \qquad (118)$$

$$e^{-\frac{s}{0.2585}} = \frac{p^2 - 1.551 p + 0.8016}{p^2 + 1.551 p + 0.8016} \qquad (119)$$

$$-T_s = 0.105 T_s - 0.105 \bar{T}_p + 0.083 \left[\frac{\Delta W_s}{10} \right] + \left[0.083 \left(\frac{\Delta W_s}{10} \right) \right] \qquad (120)$$

$$\bar{T}_p = \frac{0.1657 T_s}{p + 0.1657} + 0.2585 \frac{T_p(0) - T_p(L)}{p + 0.1657} \qquad (121)$$

The values of parameters used for the Boiler Simulation are listed in Appendix A, Section V.

- 50 -

FIG. 1: FUNCTIONAL DIAGRAM OF PLANT CONTROL SYSTEM

(ONE EQUIVALENT LOOP SHOWN)

$$N_D = K_1 W_S + K_2 \left\{ \Delta P + \frac{1}{T} \int \Delta P \, dt \right\}$$

COMPARATOR   PLANT CONTROLLER

P SET POINT
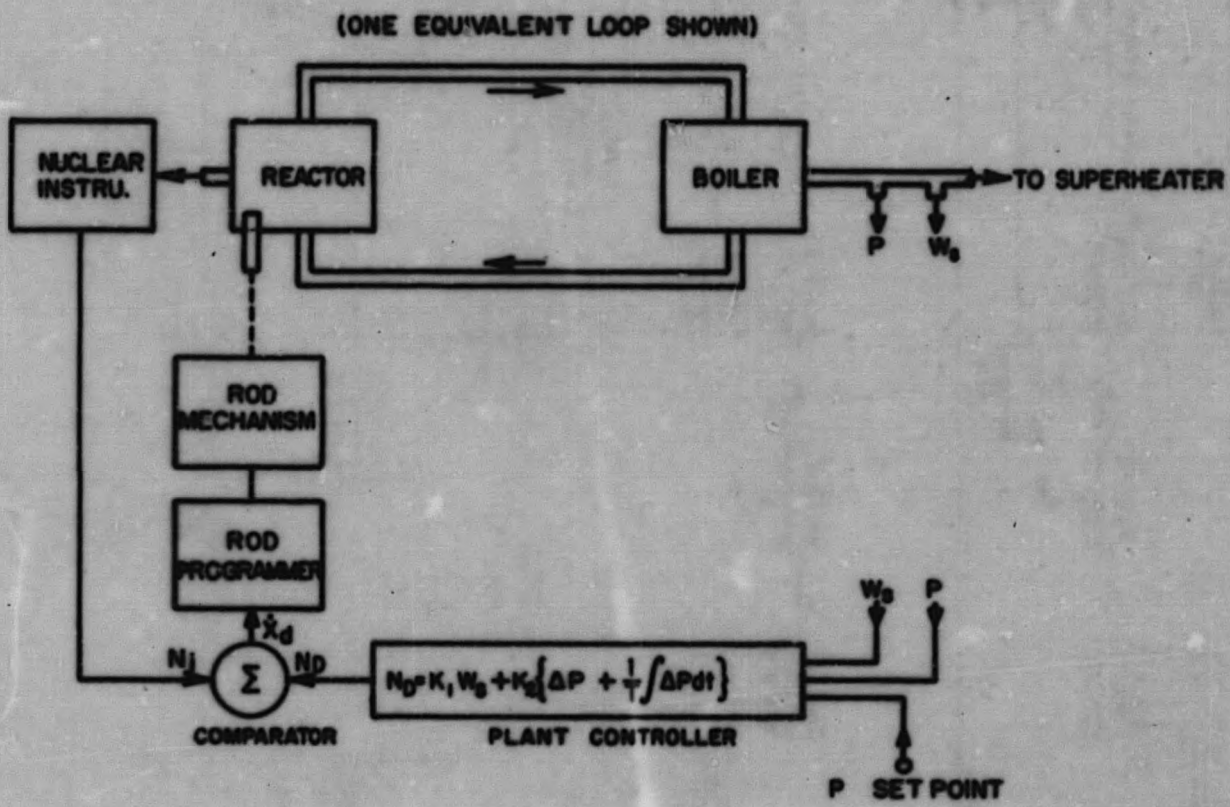
FIG. 2: CETR REACTOR PLANT CONTROLLER
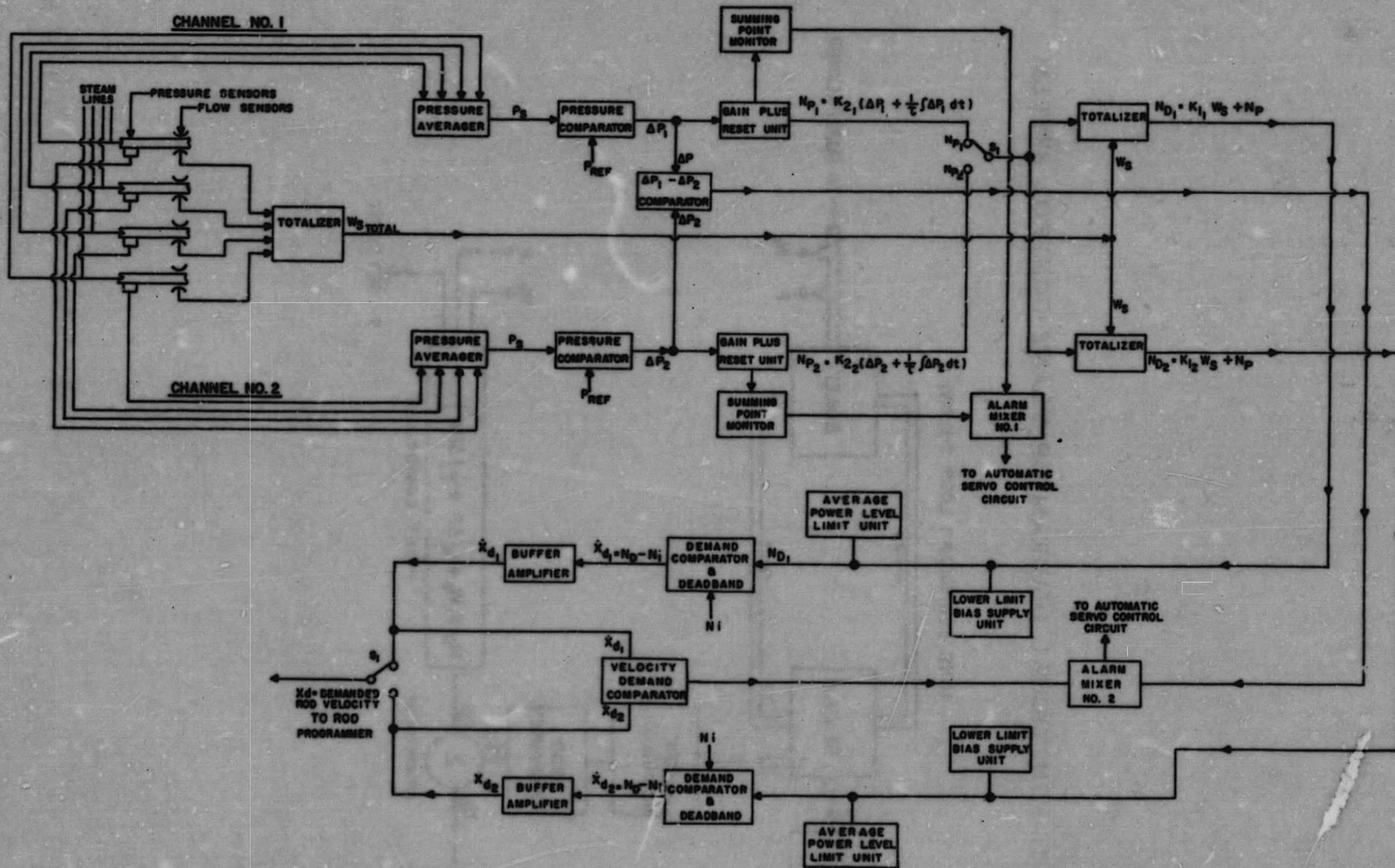
FIG. 3: DEADBAND CHARACTERISTIC

$$\Sigma = N_d - N_i$$
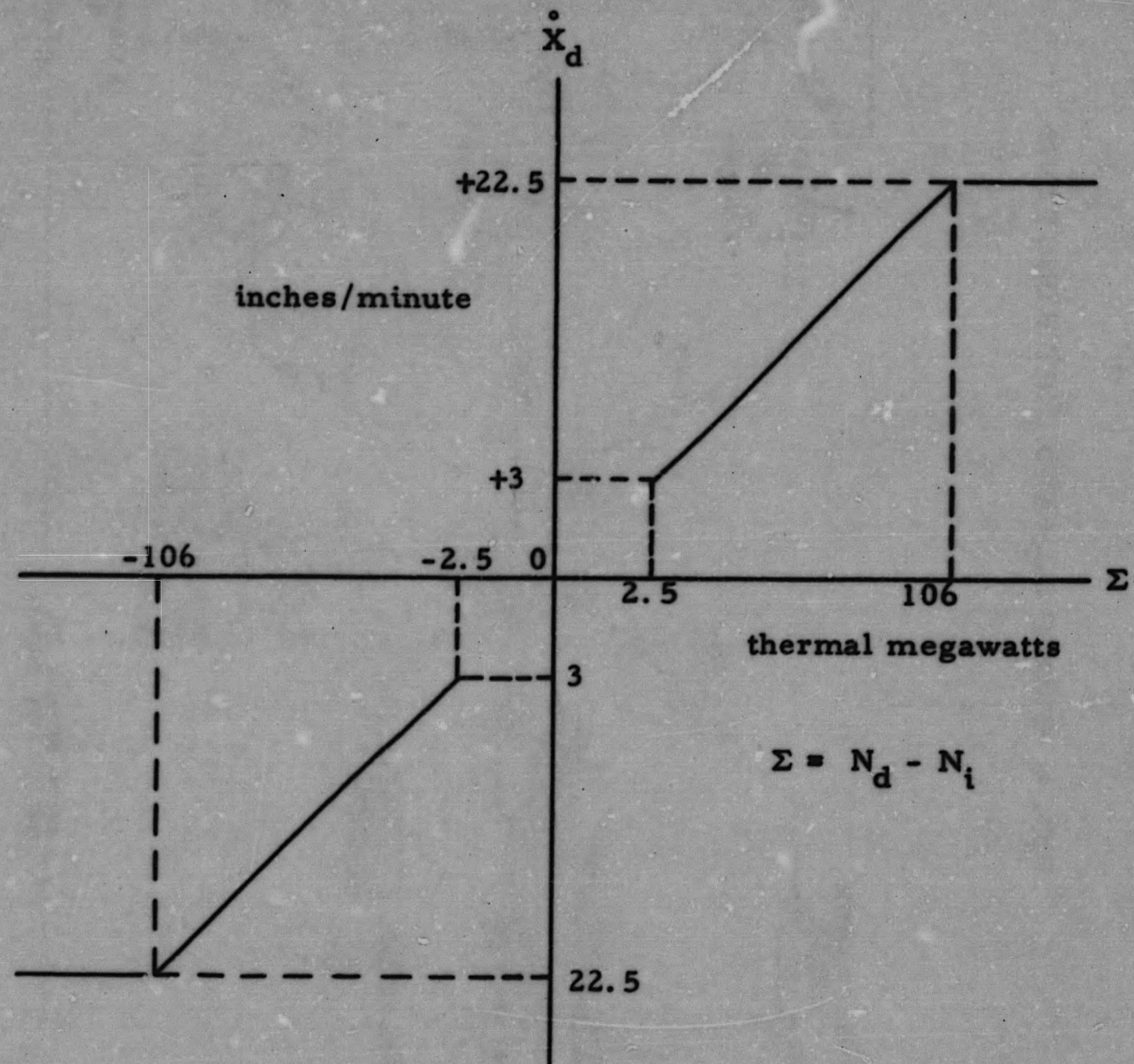
FIG. 4: GROUP DEMAND UNIT FUNCTIONS
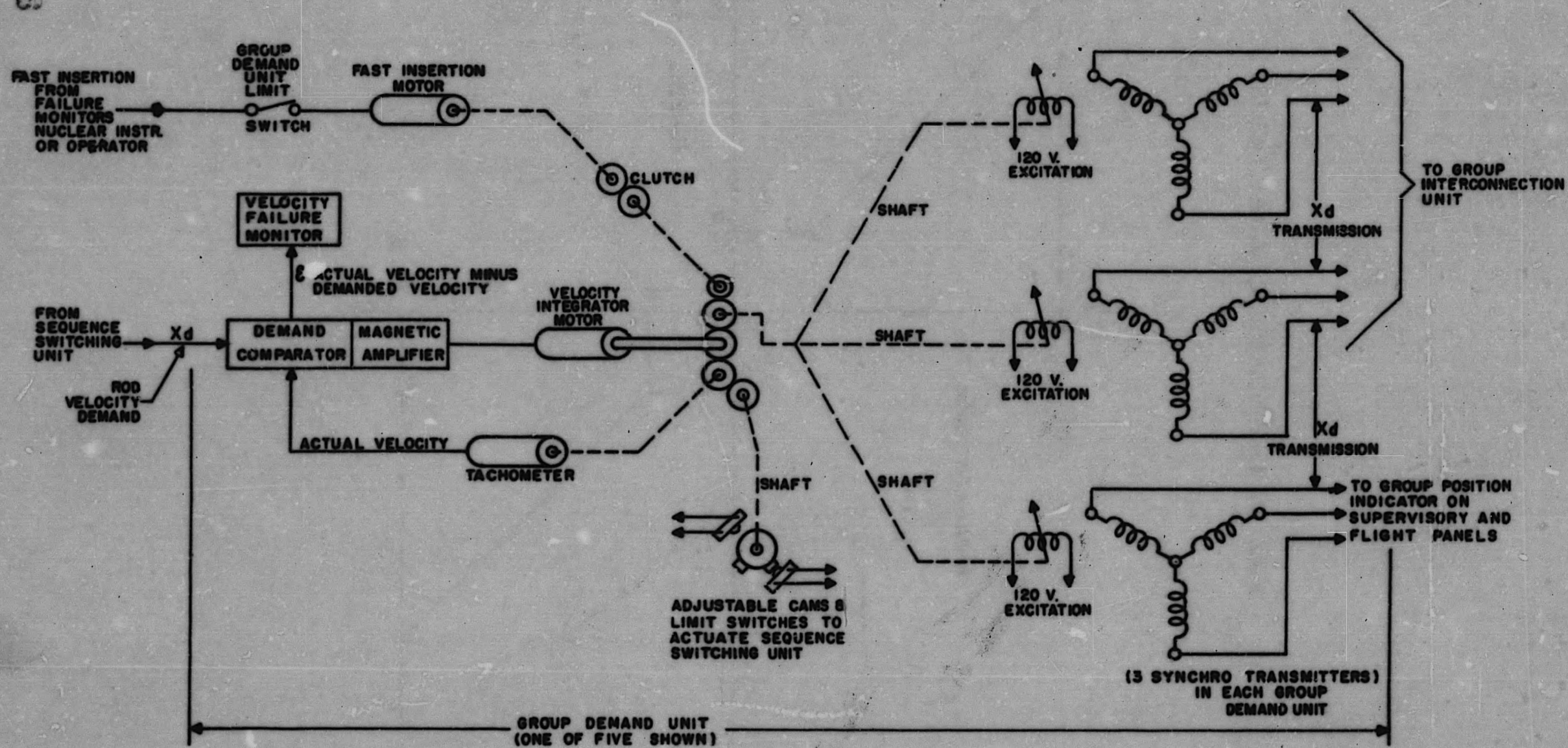
FIG. 5: ROD SERVOMECHANISM SYSTEM

SERVO ROD. MECHANISM SYSTEM
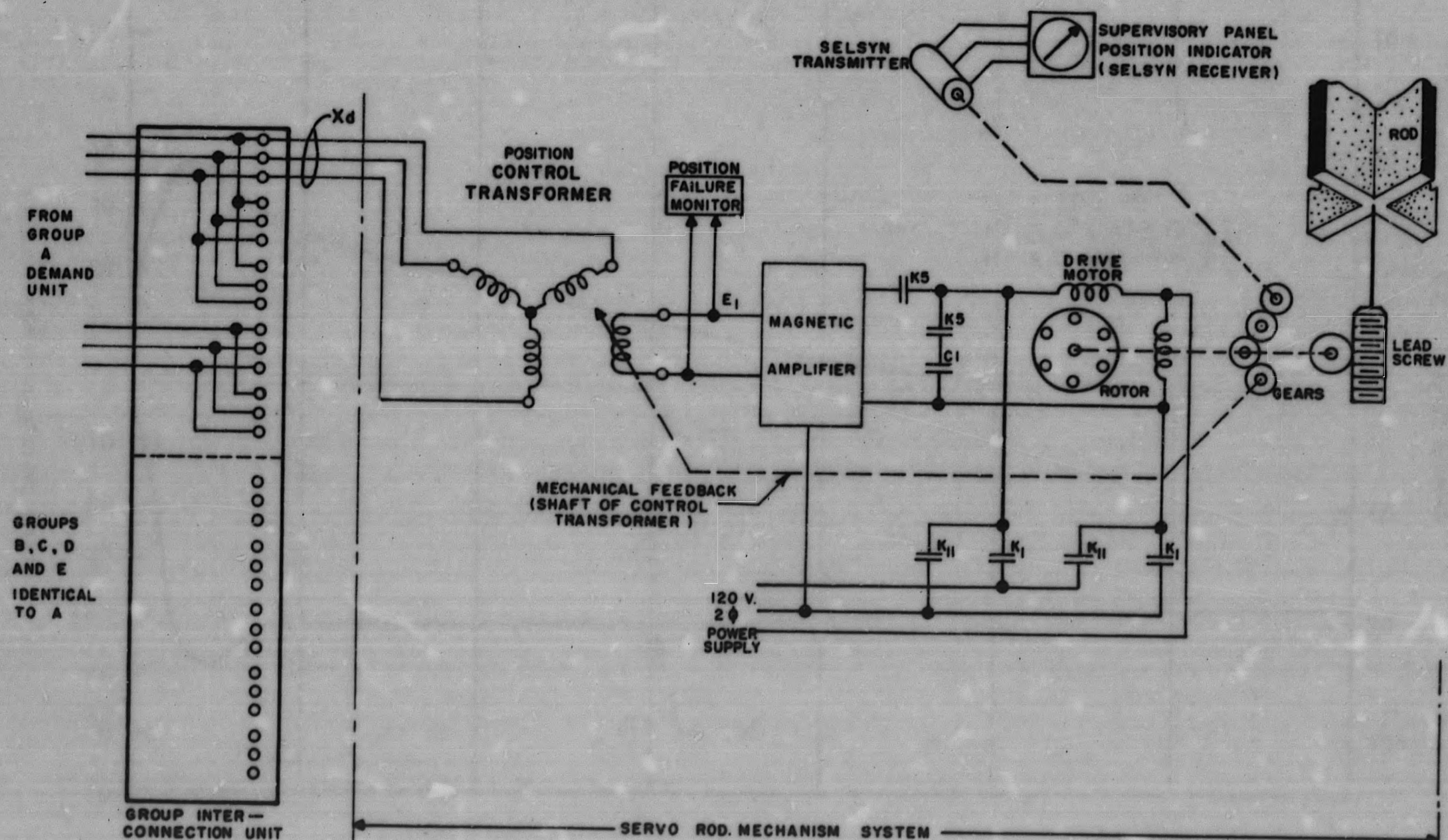
C-I: Phase Shift Capacitor

NOTE:
It is not Possible to Energize the KI Withdraw or KII Insert Relays When the K5 Group Relay is Energized.

K5
Contacts are Closed When the Group Control Relay is Energized.

KI
Contacts are Closed When the Withdraw Relay is Energized.

KII
Contacts are Closed When the Insert Relay is Energized.

FIG. 6: PLANT RESPONSE TO + 18. 2% STEP STEAM LOAD
CHANGE — BEGINNING OF CORE LIFE

$K_1 = 0.85$ sec/lb
$K_2 = 0.0015$ in.^{2}/lb
$\tau = 200$ sec
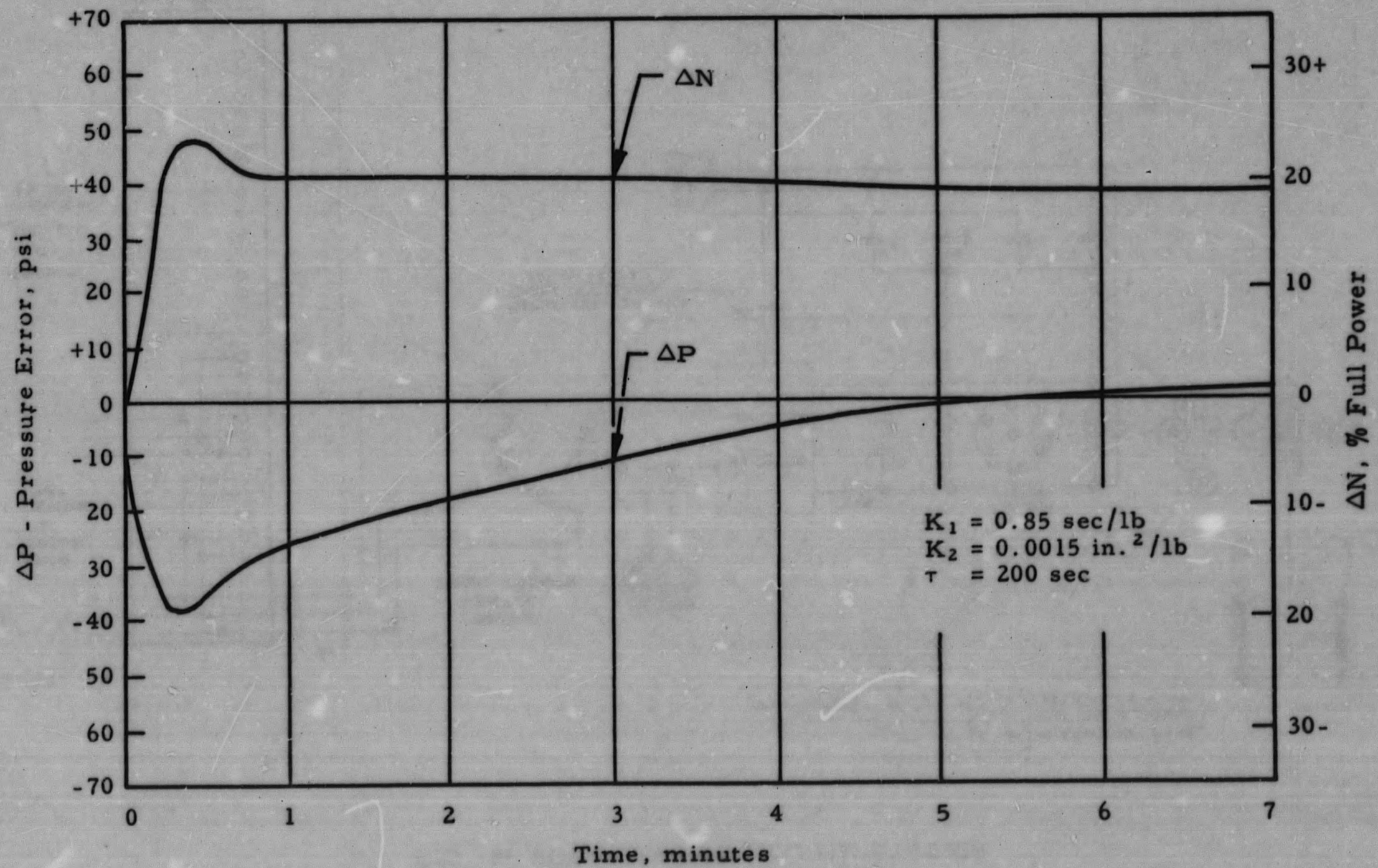
FIG. 7: PLANT RESPONSE TO -18.2% STEP STEAM
LOAD CHANGE — BEGINNING OF CORE LIFE

FIG. 8: PLANT RESPONSE TO +9.1% PER MINUTE STEAM
LOAD CHANGE — BEGINNING OF CORE LIFE
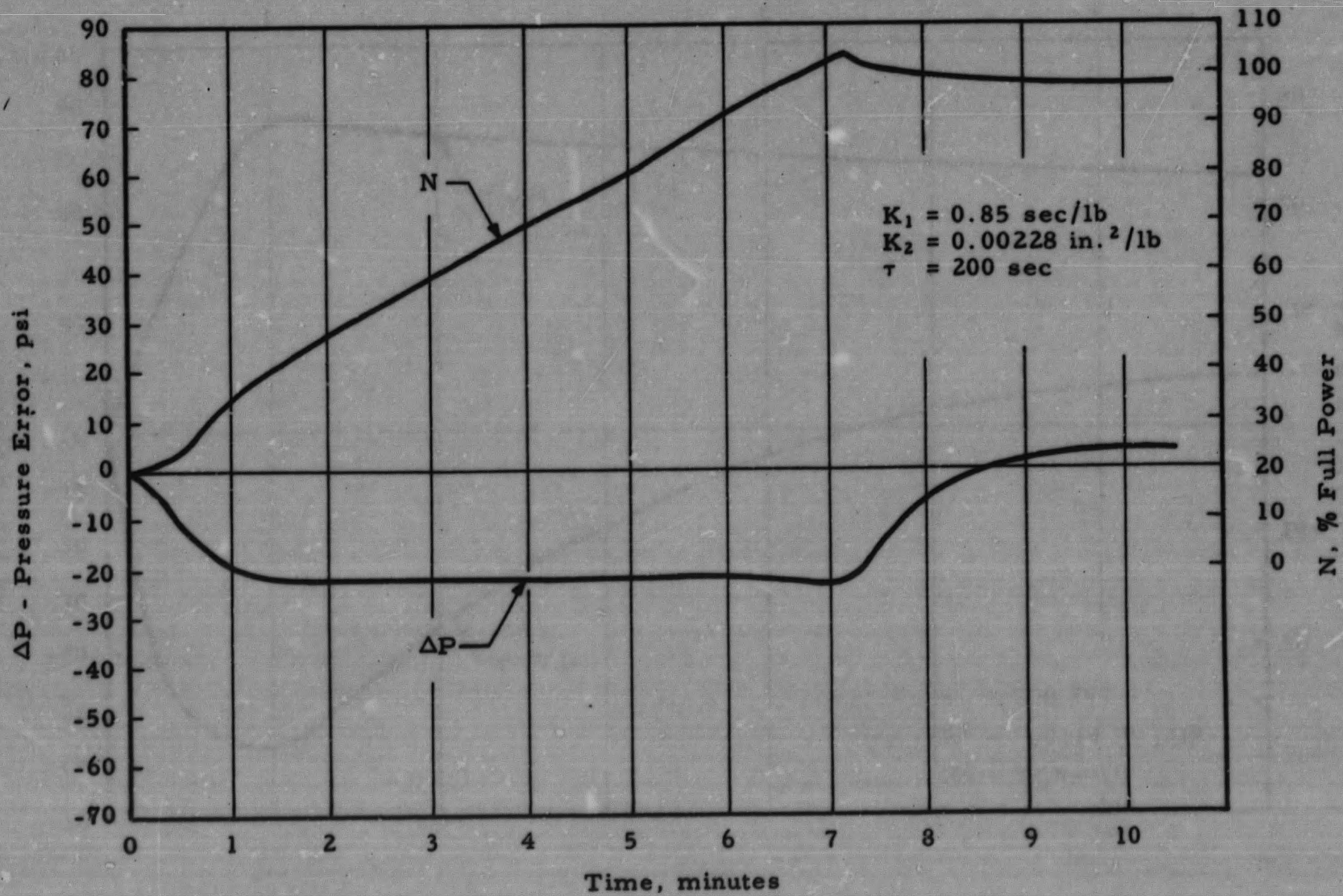
$K_1 = 0.85$ sec/lb
$K_2 = 0.00228$ in.^{2}/lb
$\tau = 200$ sec

FIG. 9: PLANT RESPONSE TO -9.1% PER MINUTE STEAM
LOAD CHANGE — BEGINNING OF CORE LIFE

$K_1 = .85$ sec/lb

$K_2 = .00228$ in.^{2}/lb

$\tau = 200$ sec.
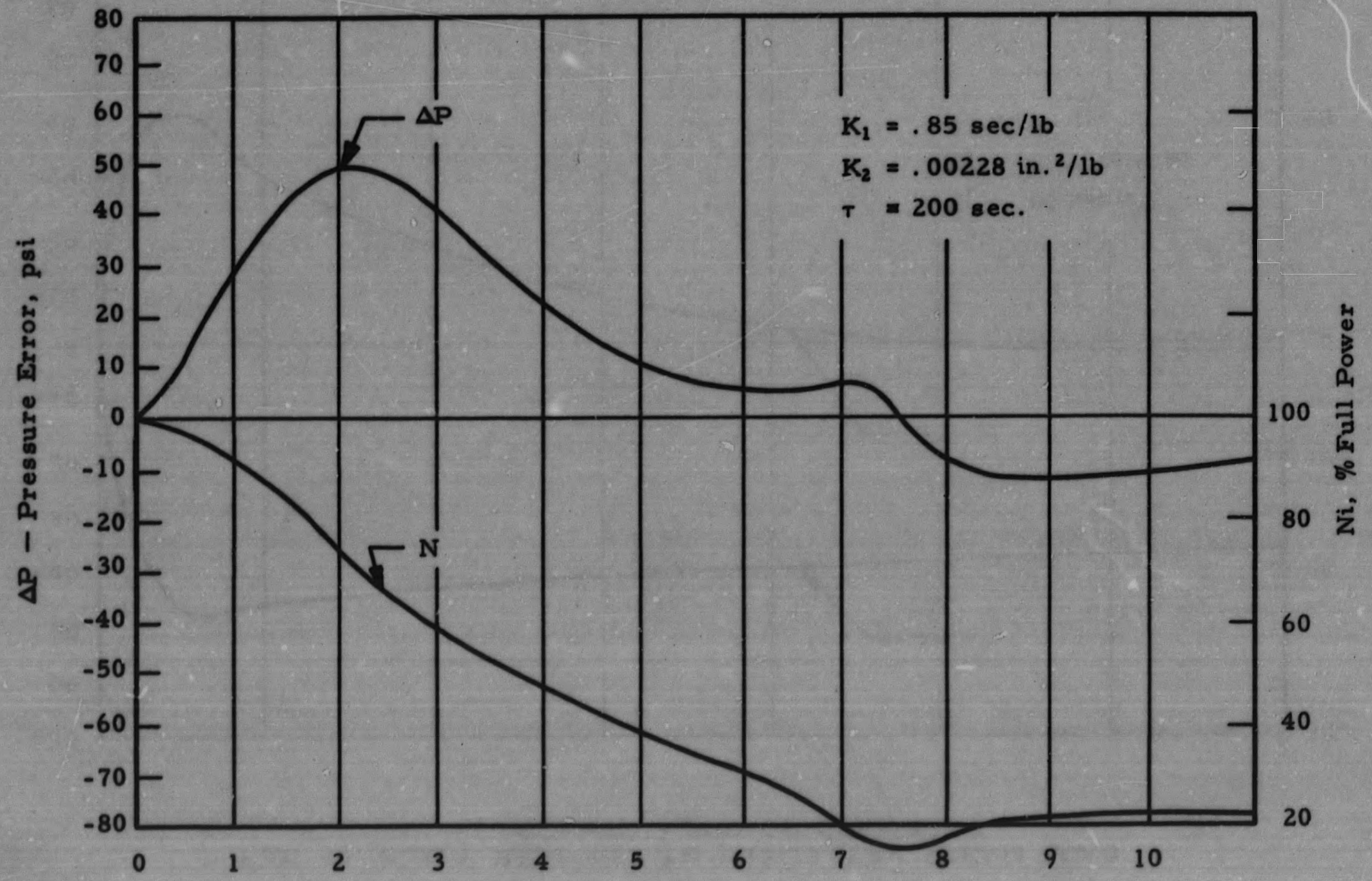
FIG. 10: PLANT RESPONSE TO +18.2% STEP STEAM LOAD
CHANGE — END OF CORE LIFE

K_1 = .85 sec/lb
K_2 = .0015 in.^{2}/lb
τ = 200 sec
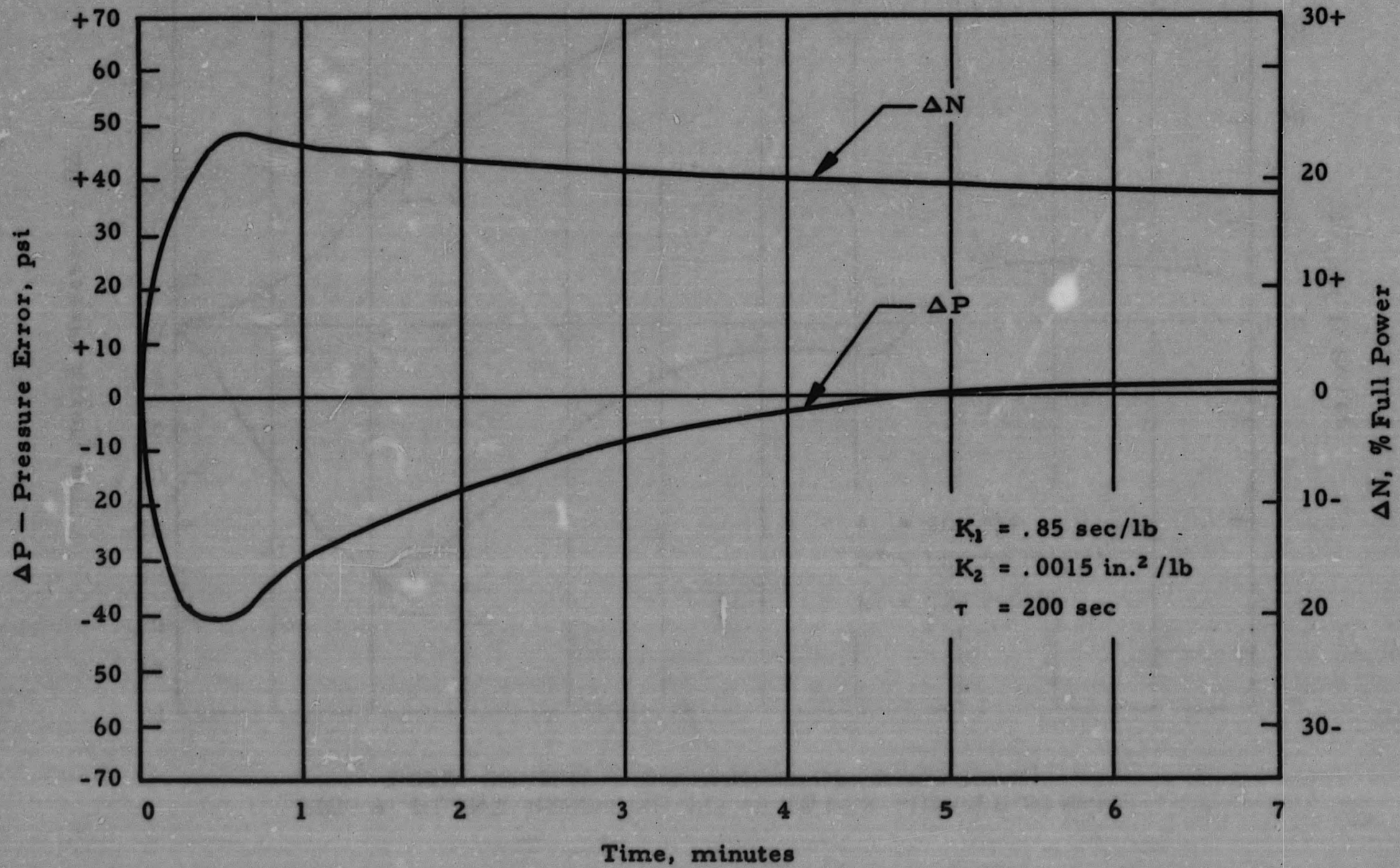
FIG. 11: PLANT RESPONSE TO + 18.2% STEP STEAM LOAD CHANGE — END OF CORE LIFE
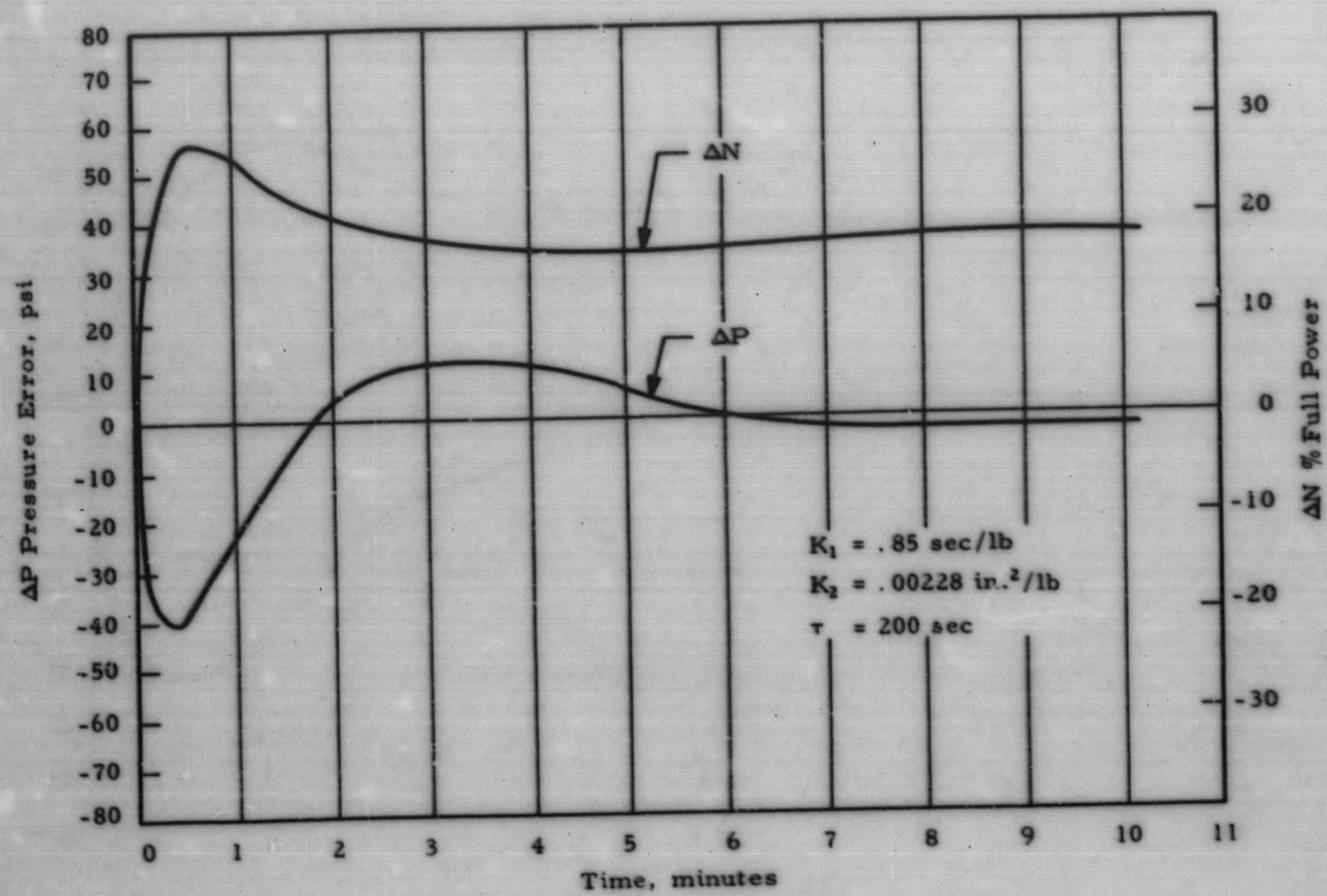
FIG. 12: PLANT RESPONSE TO -18.2% STEP STEAM LOAD CHANGE — END OF CORE LIFE
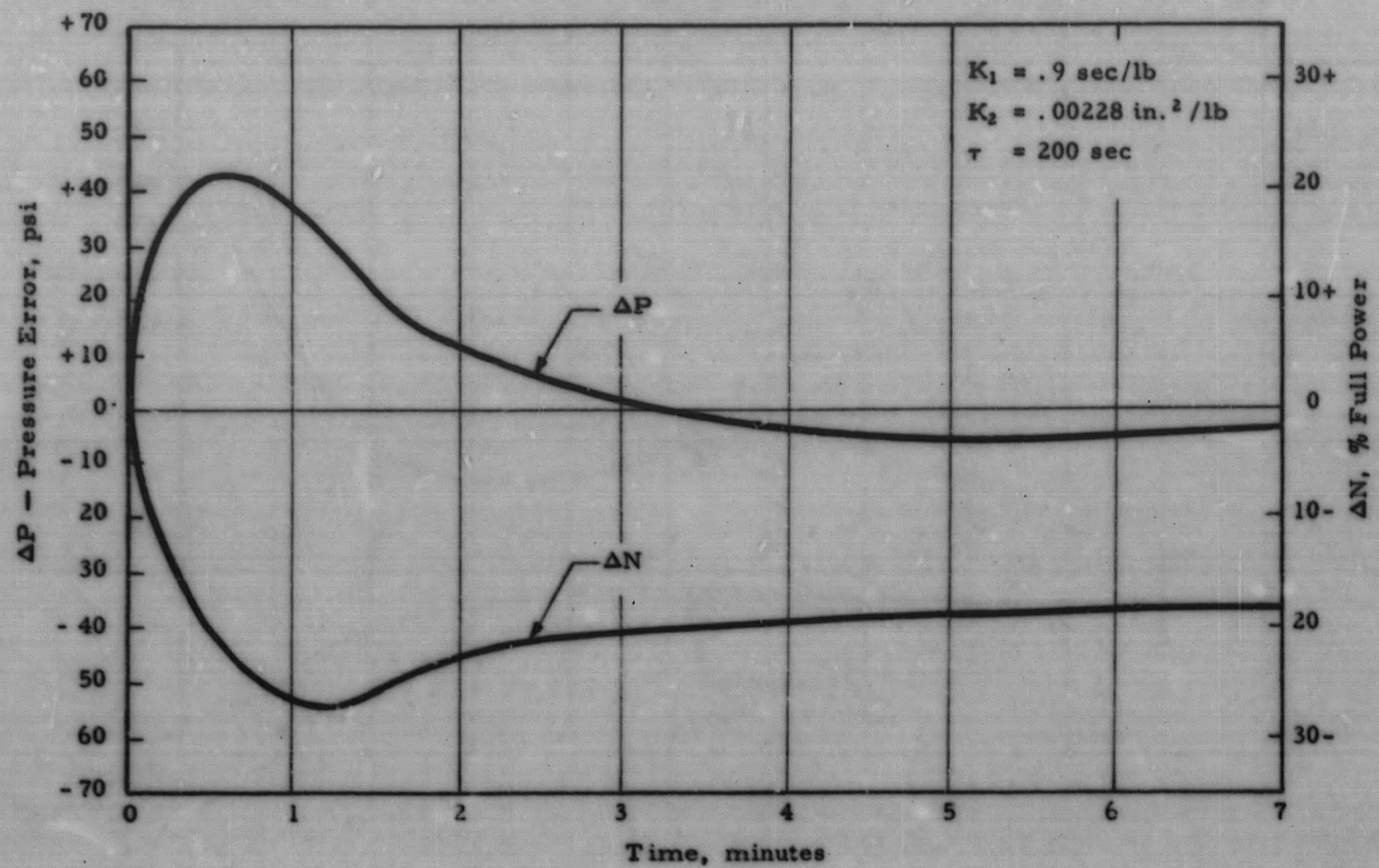
FIG. 13: PLANT RESPONSE TO + 9.1% PER MINUTE STEAM
LOAD CHANGE — END OF CORE LIFE
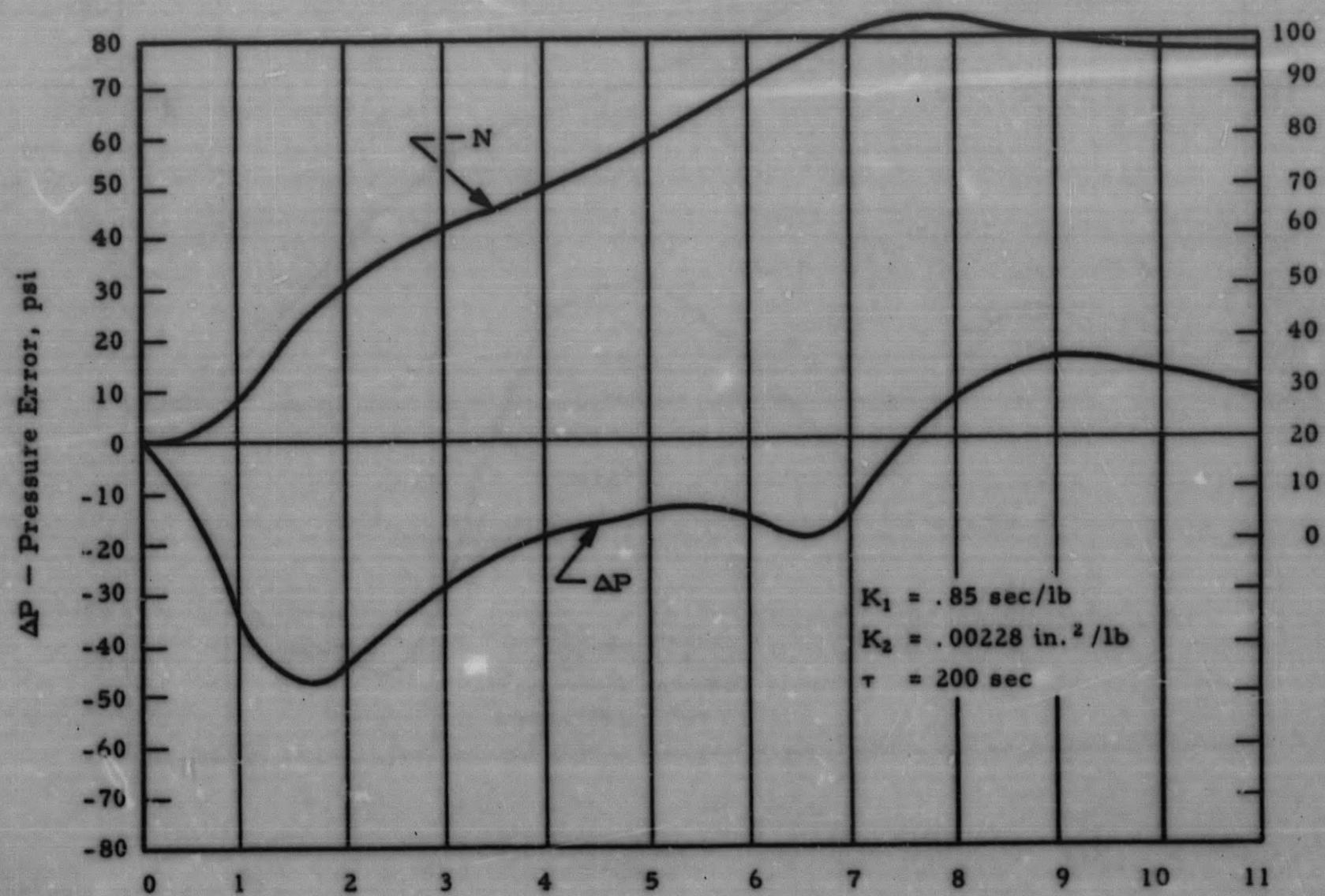
FIG. 14: PLANT RESPONSE TO -9.1% PER MINUTE STEAM LOAD CHANGE — END OF CORE LIFE
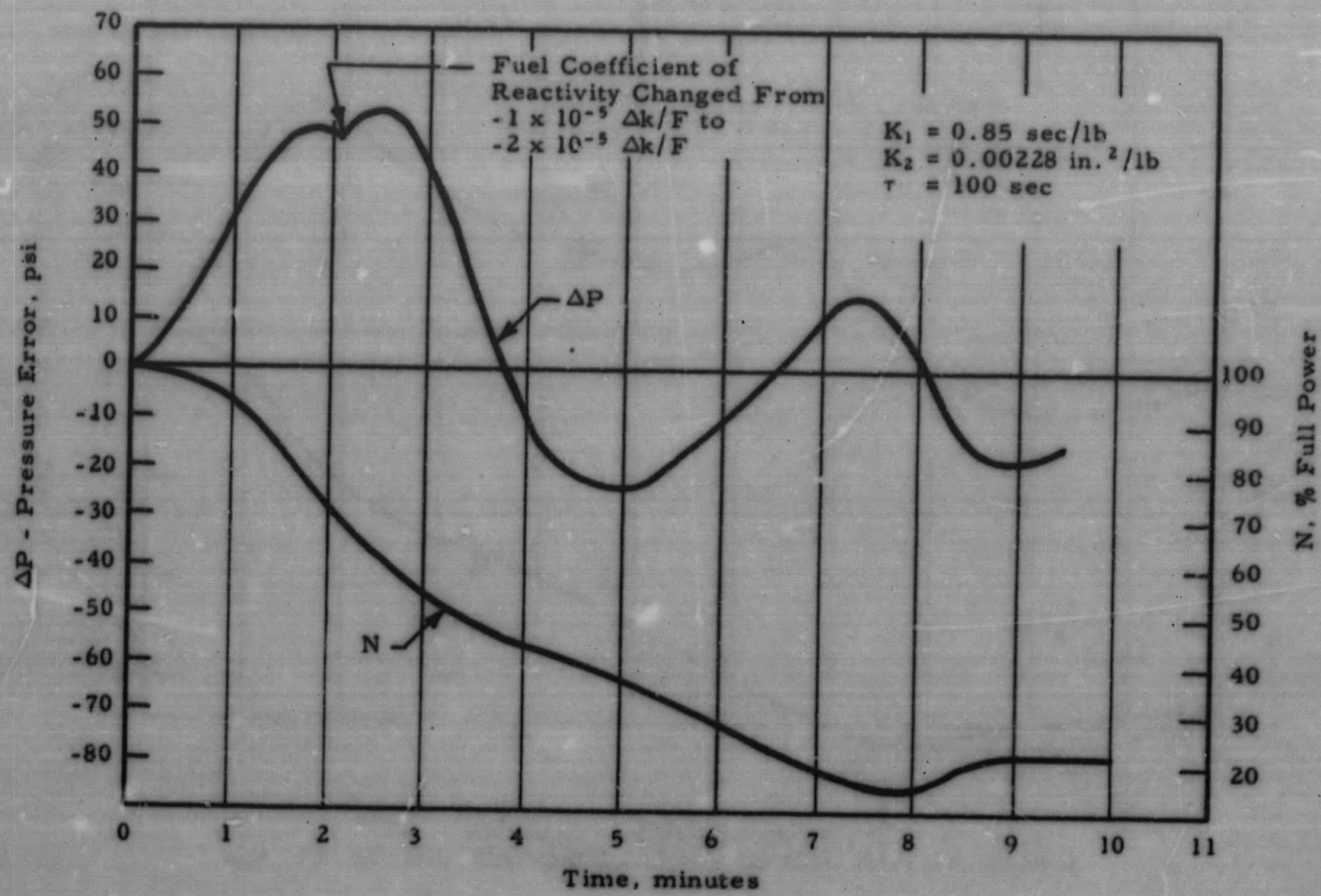
FIG. 15: POWER OVERSHOOT Vs K_2 SETTING
(Step Steam Demand)
$K_1 = .85$ sec/lb
$d_f = -1 \times 10^{-5}$ $\Delta k/F$
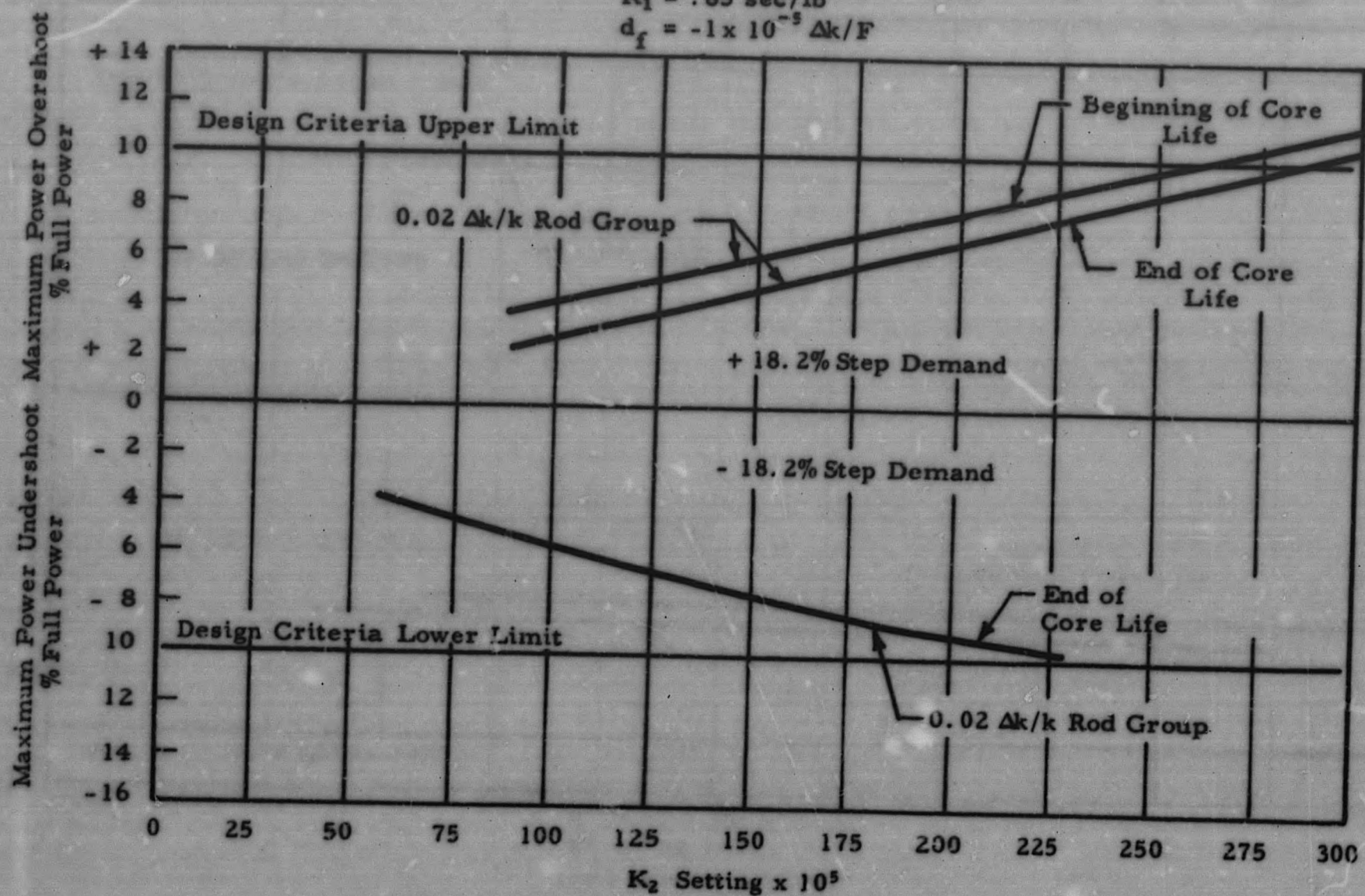
FIG. 16: PRESSURE ERROR Vs K_2 SETTING
(Step Steam Demand)
$K_1 = .85$ sec/lb
$d_f = -1 \times 10^{-5}\ \Delta k/F$
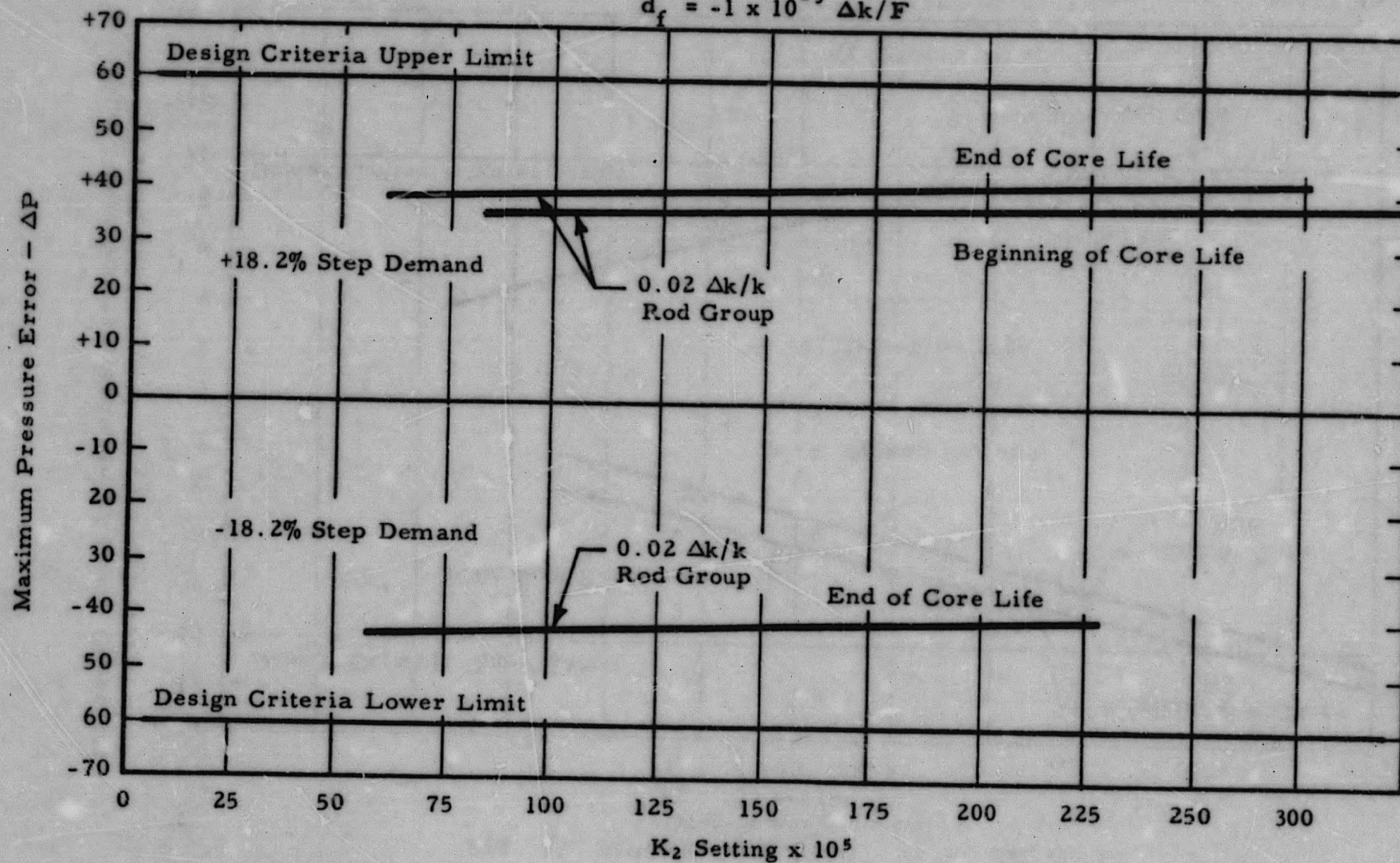
FIG. 17: REACTOR KINETICS SIMULATION

(Simulation of Equations 5,6,9, Appendix B)

FIG. 18: DIFFERENTIAL ROD WORTH CURVE

$\dfrac{\partial \rho}{\partial x}$

50.2 x 10⁻⁵ Δk/in.

(2% Rod Group Illustrated)

7.75 x 10⁻⁵ Δk/in.

Rod Group Position, in.
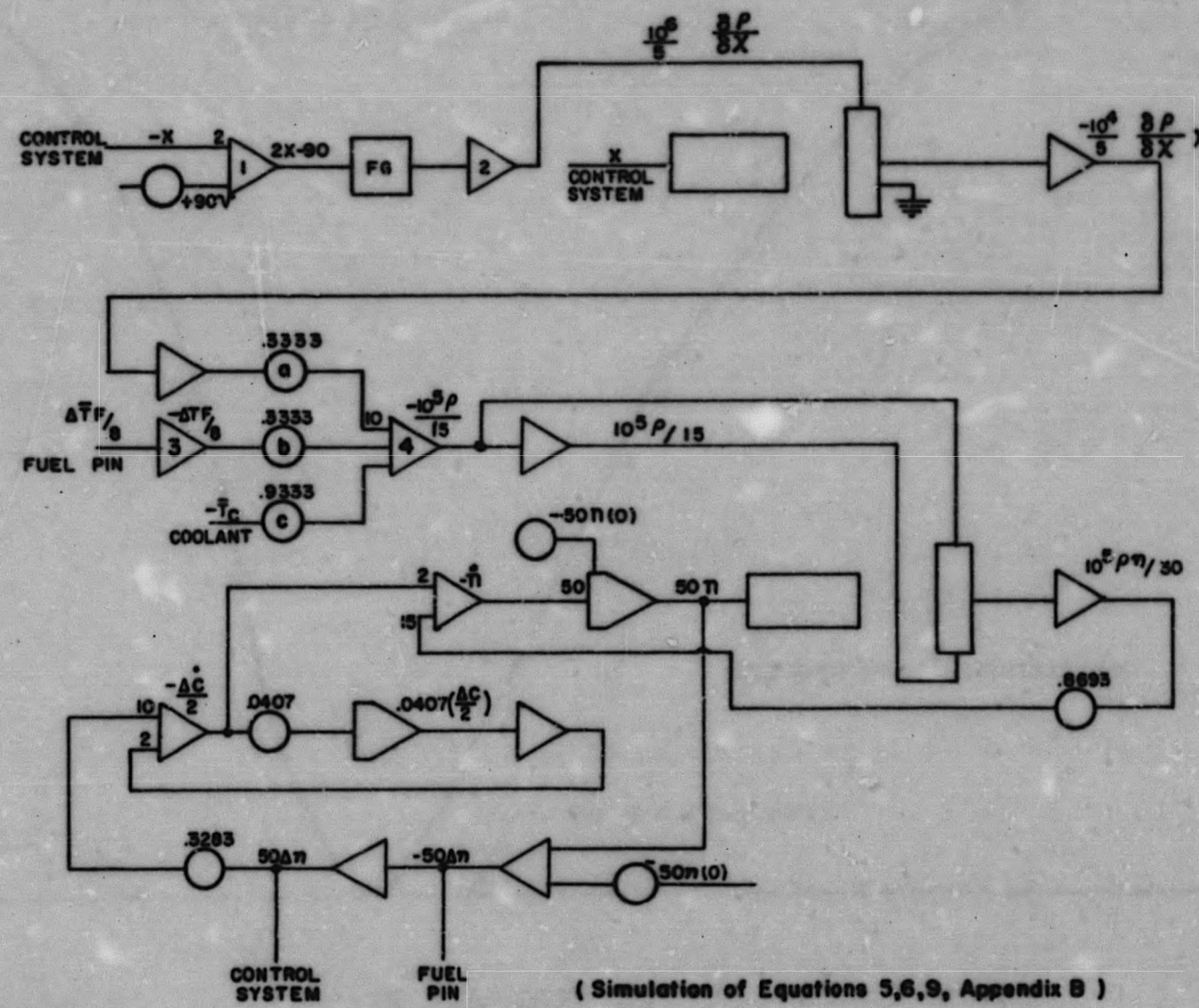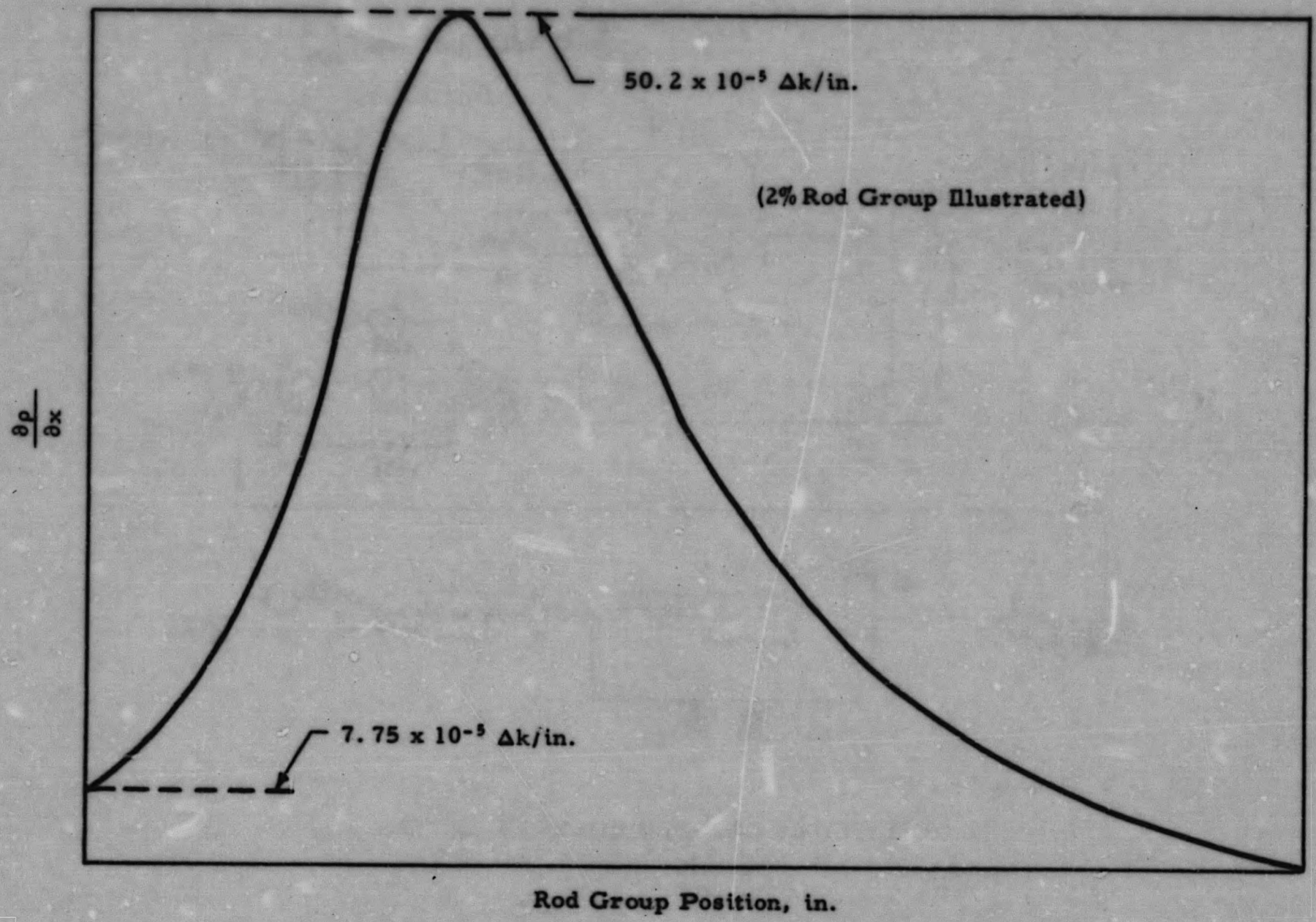
FIG. 19: CETR CONTROL ROD WORTH CURVE

Rod Group Worth (Per Cent of Fully Inserted Worth) vs. Rod Group Insertion Distance, per cent

Fully Inserted
Worth = 0.02 Δk

Fully Inserted
Worth = 0.042 Δk
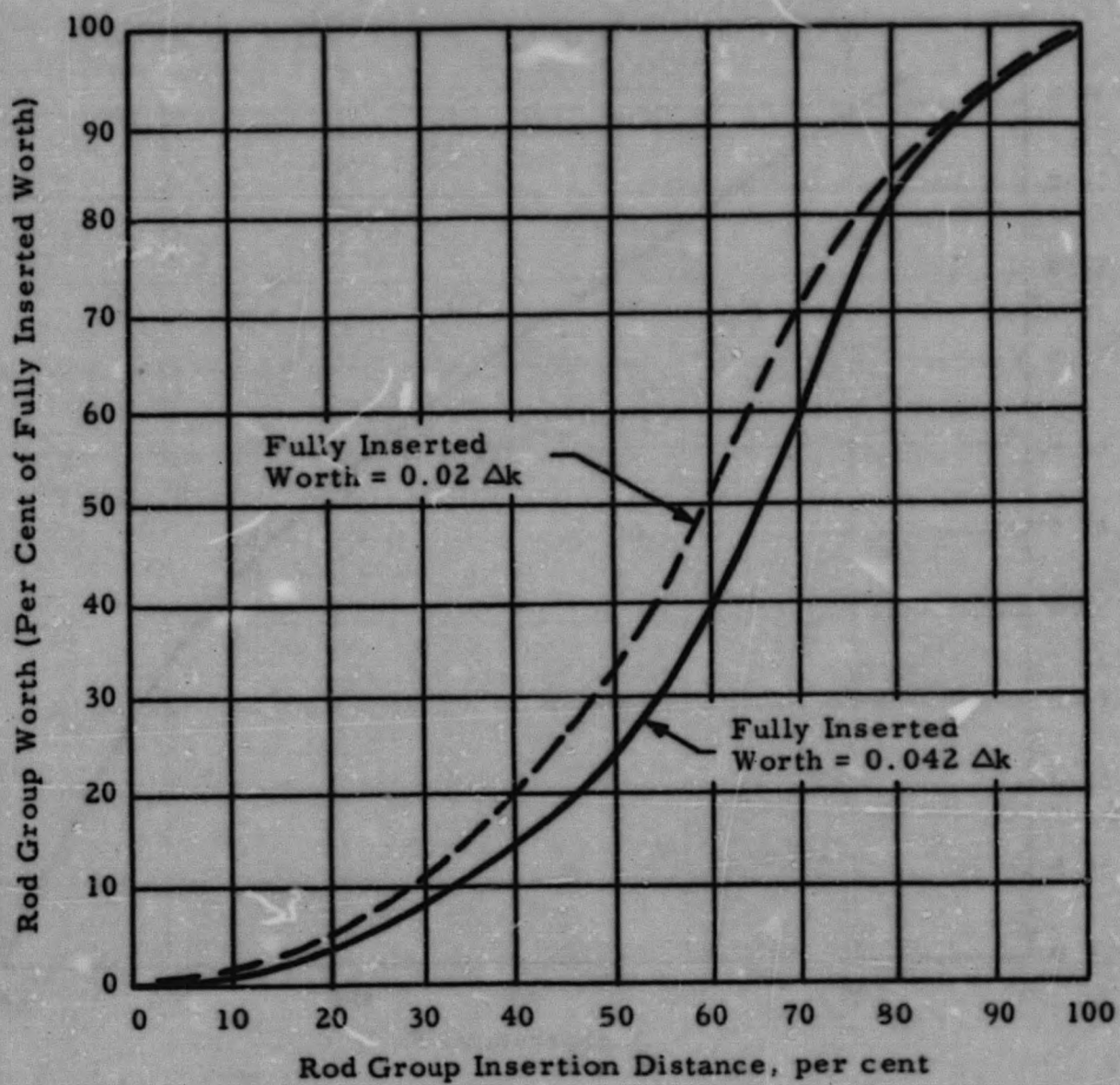
FIG. 20: CHANGE IN CORE REACTIVITY Vs TEMPERATURE

$1.4 \times 10^{-4} \, \Delta k / \degree F$

y-axis: $\Delta k_{eff}/k_{eff}$, %

x-axis: Temperature, F
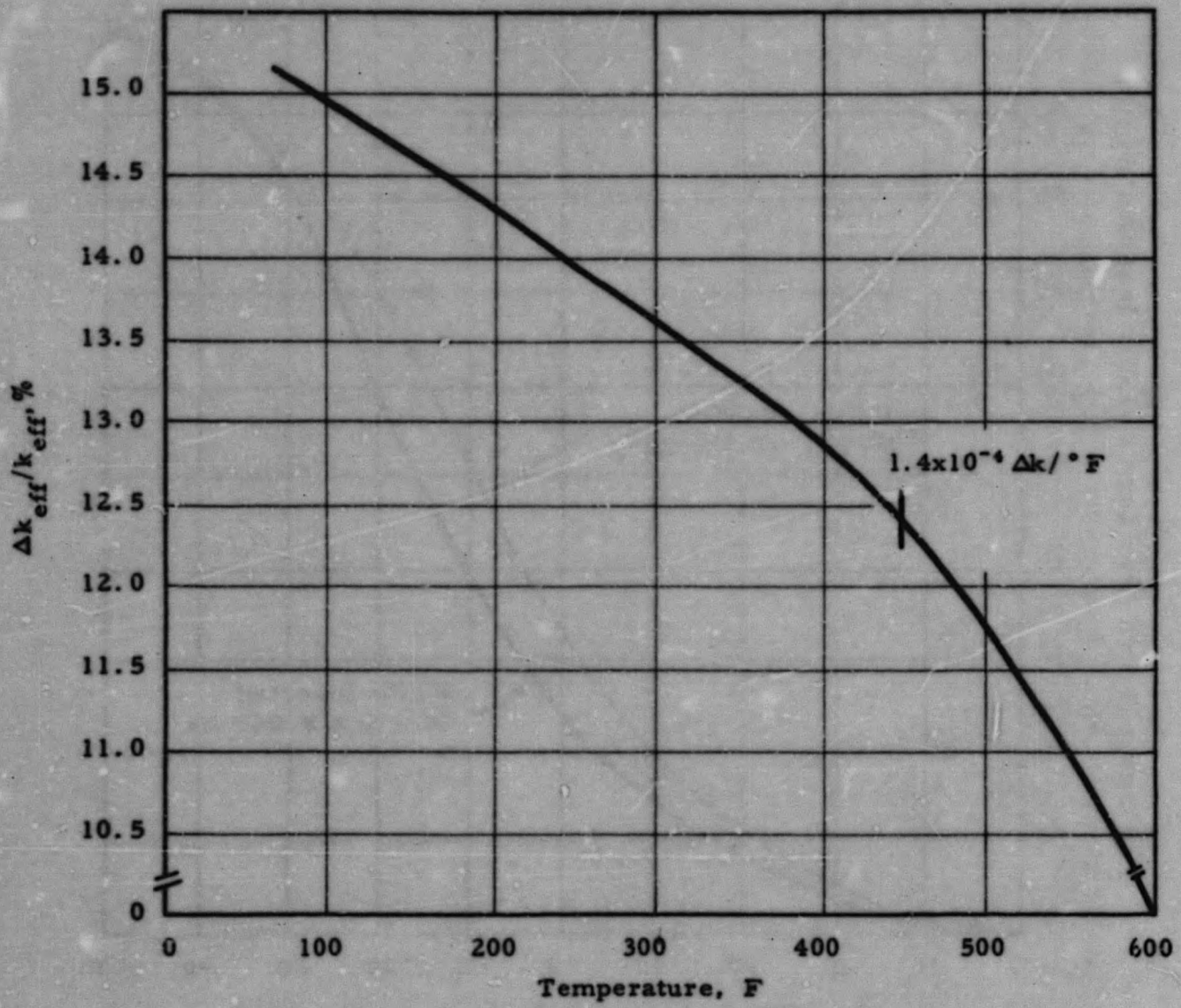
FIG. 21: CHANGE IN CORE REACTIVITY Vs FUEL
TEMPERATURE AND POWER
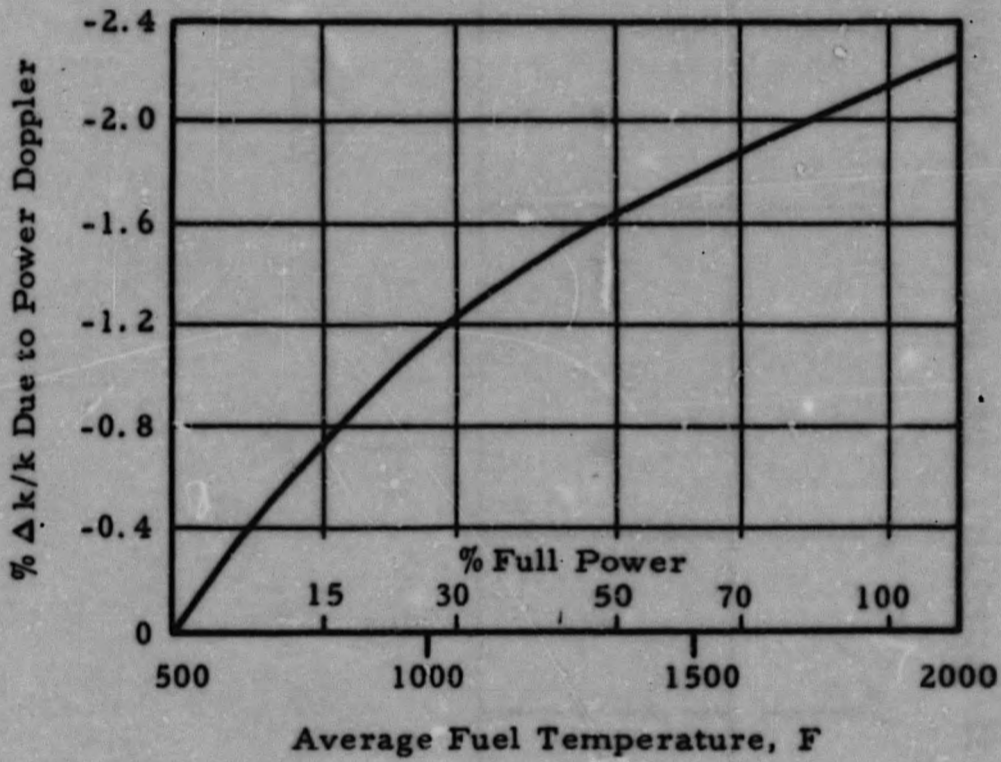
FIG. 22: AVERAGE FUEL PIN FINITE DIFFERENCE MODEL
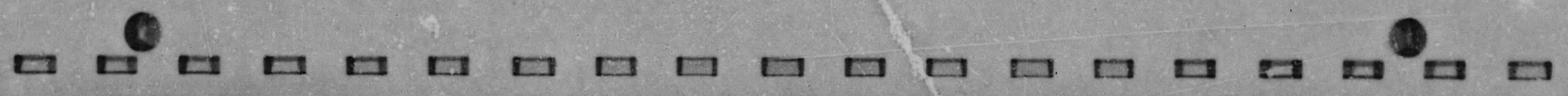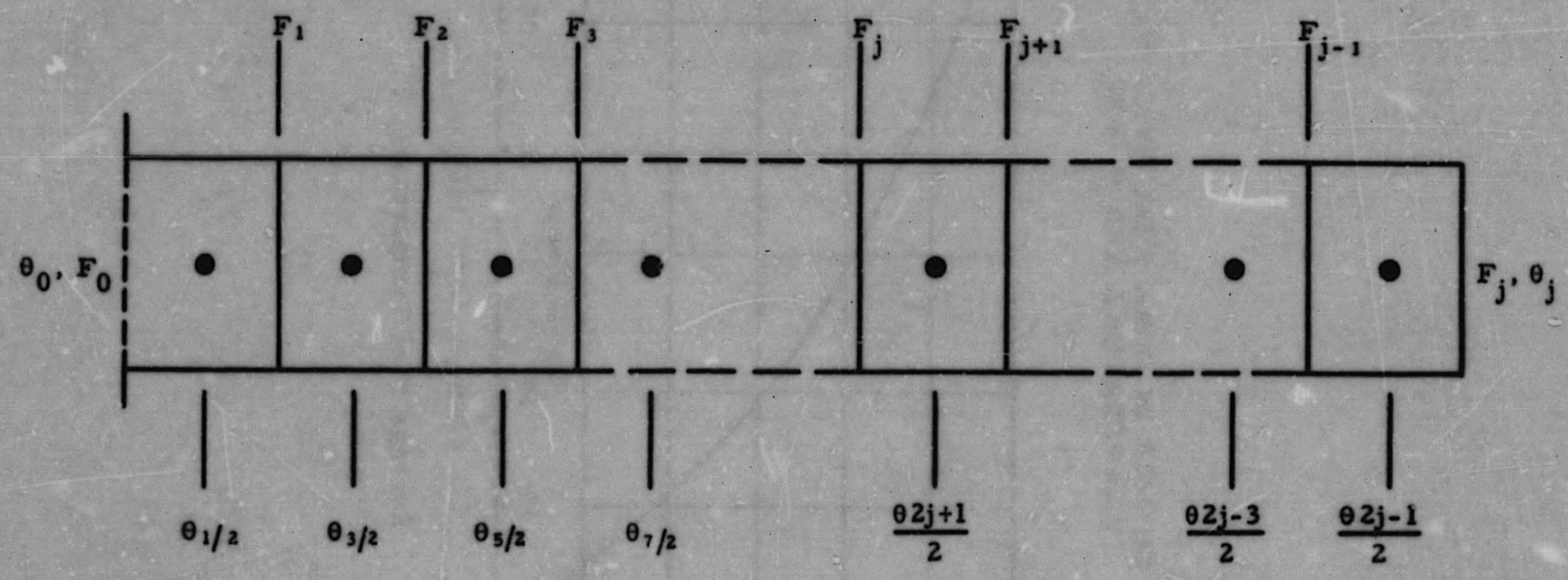
FIG. 23: CLAD TEMPERATURES
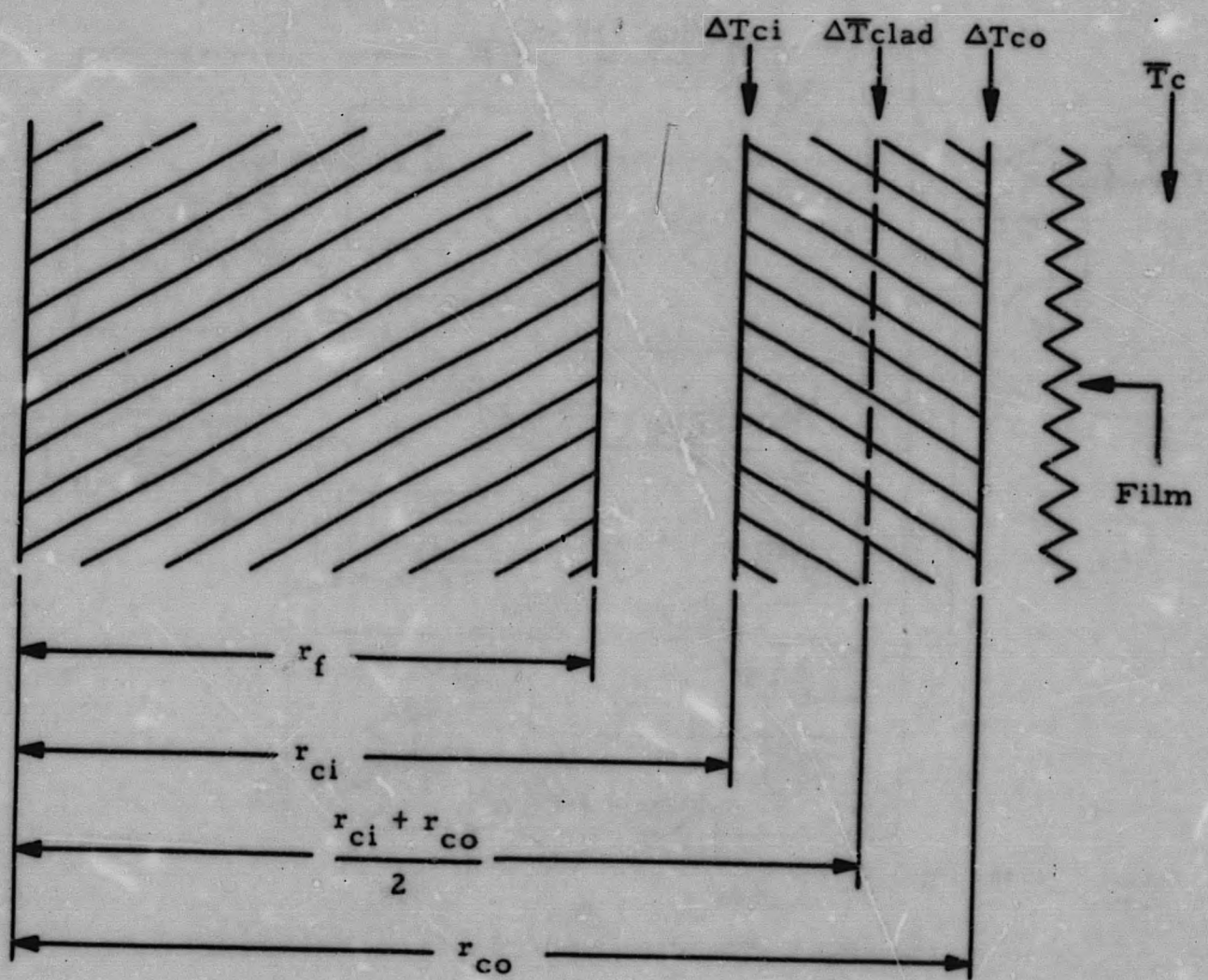
FIG. 24: FUEL ROD SIMULATION
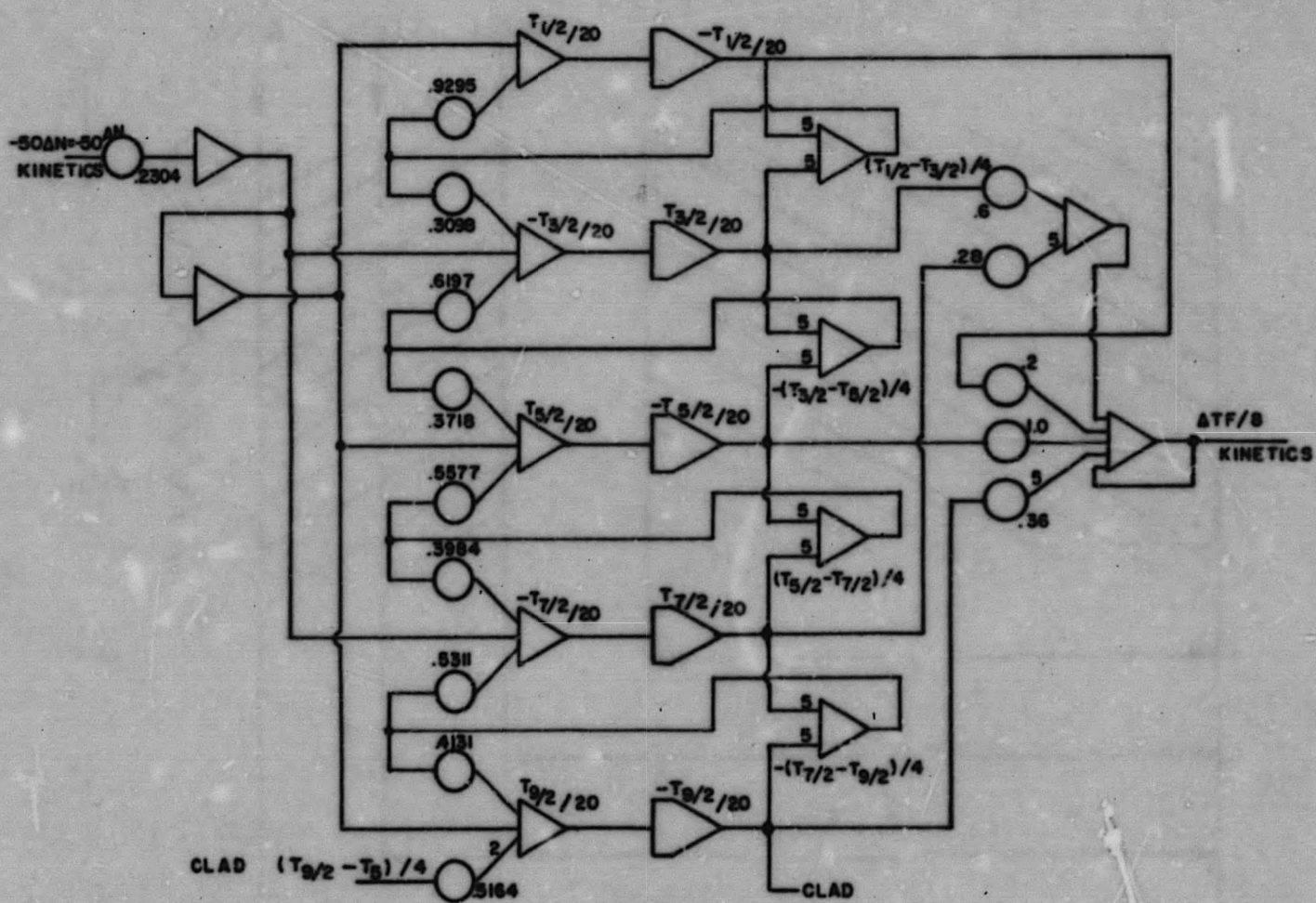
(Simulation of Equations 30, 32, 33, 34, Appendix B)

78

FIG. 25: CLAD SIMULATION
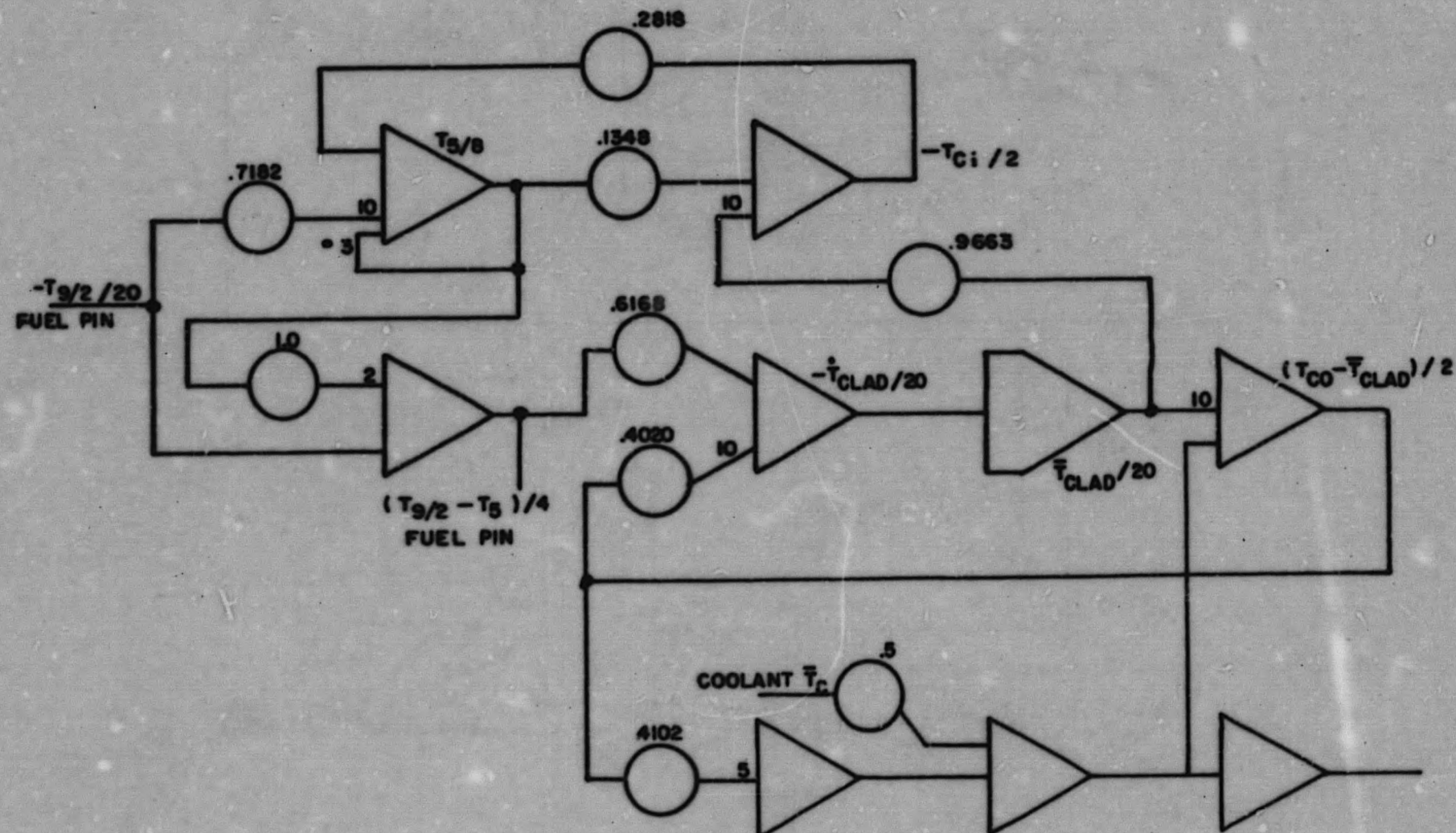
(Simulation of Equations 35, 36, 37, 40 — Appendix B)

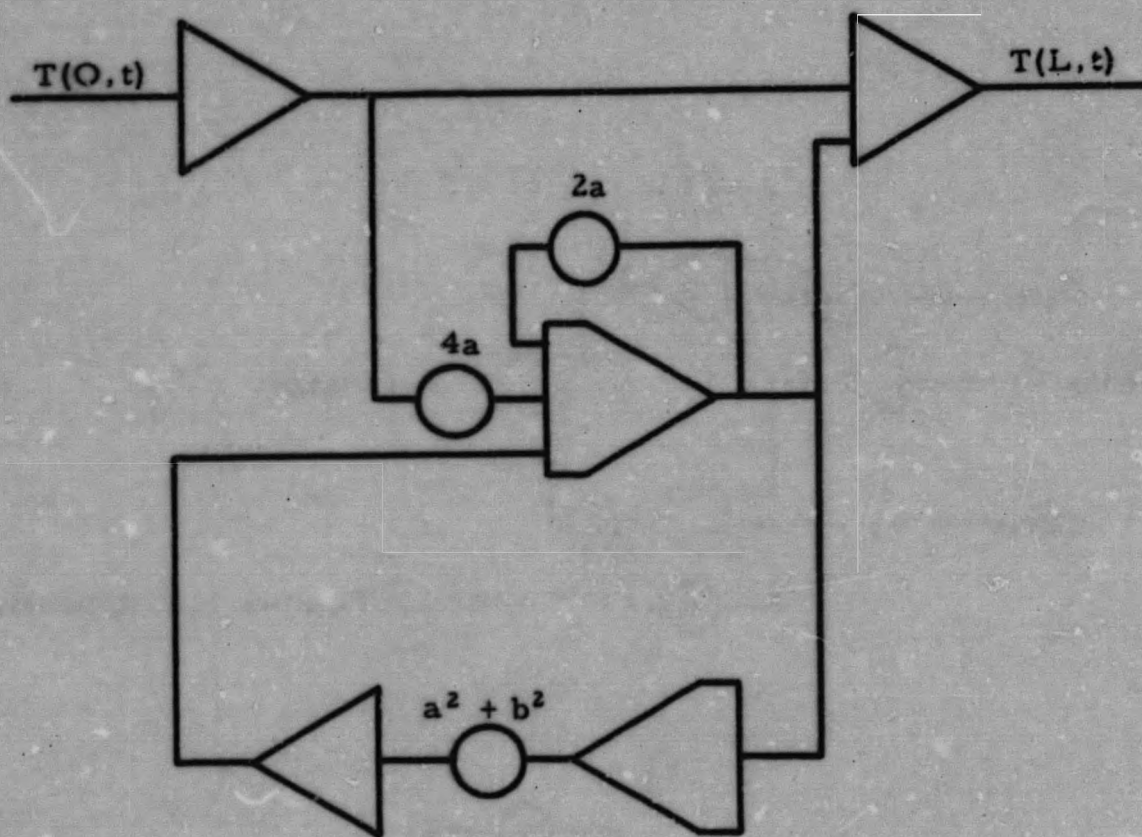FIG. 26: COOLANT SIMULATION

(Simulation of Equations
61, 62 – Appendix B)
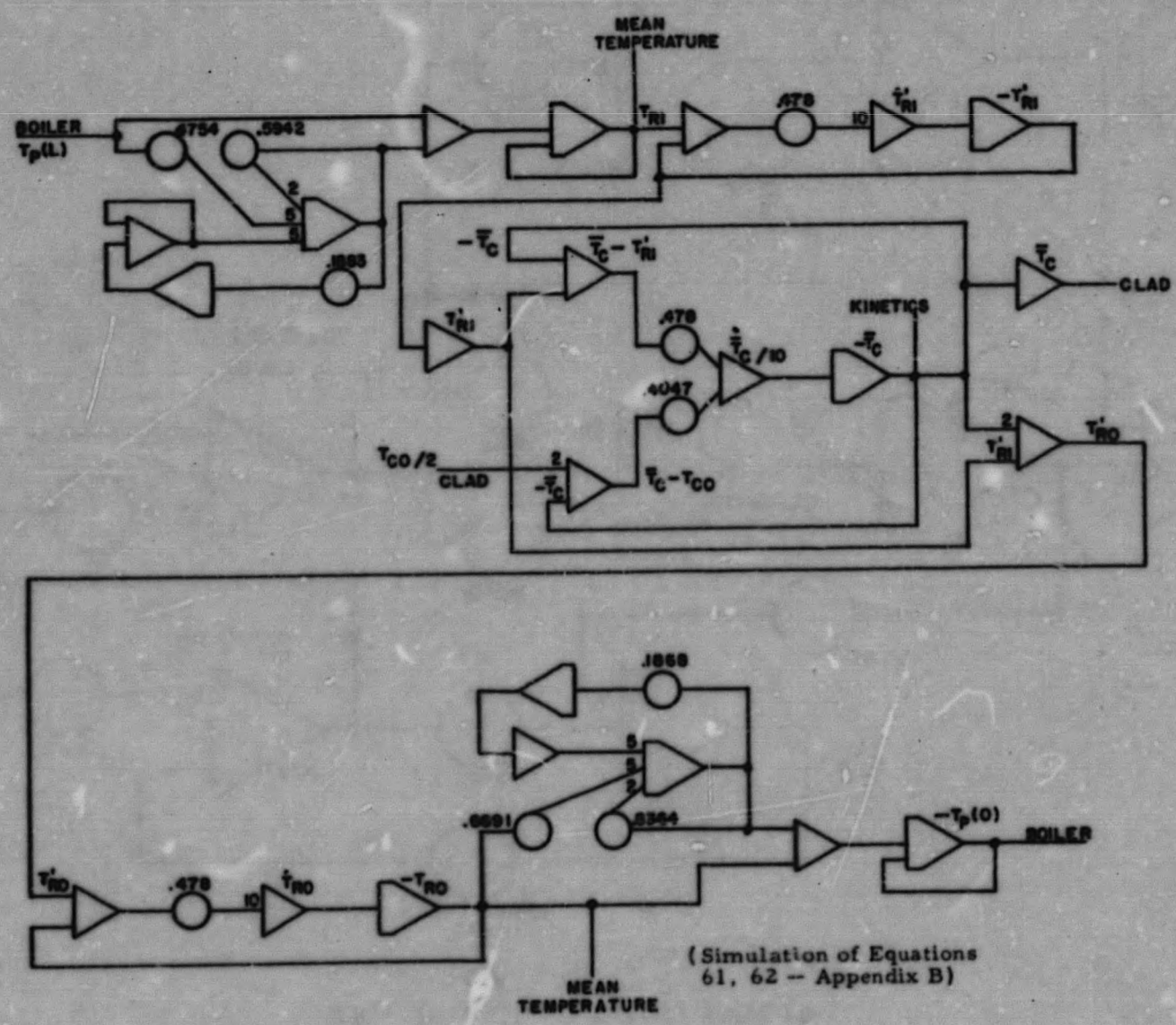
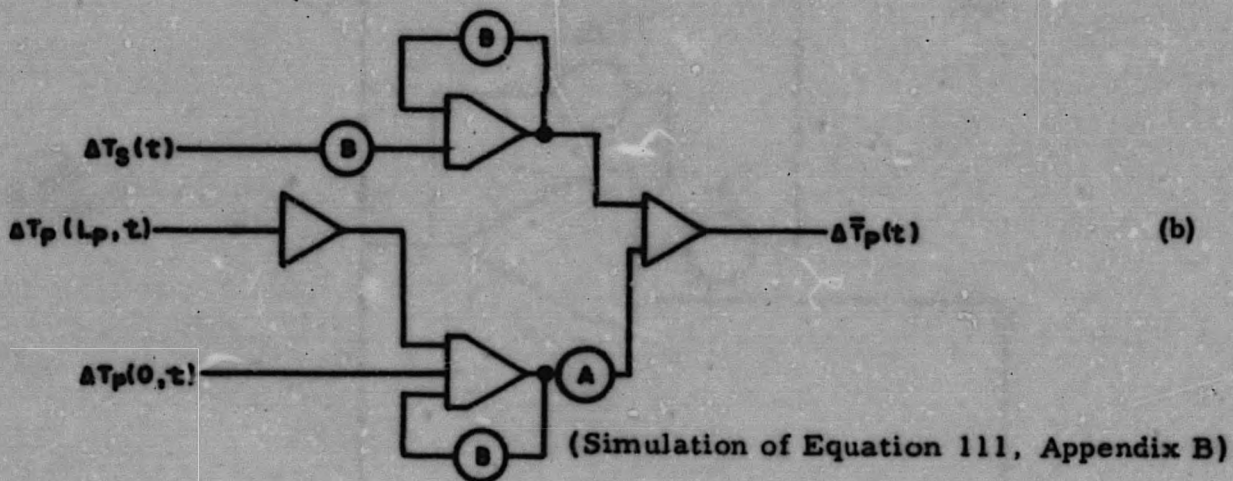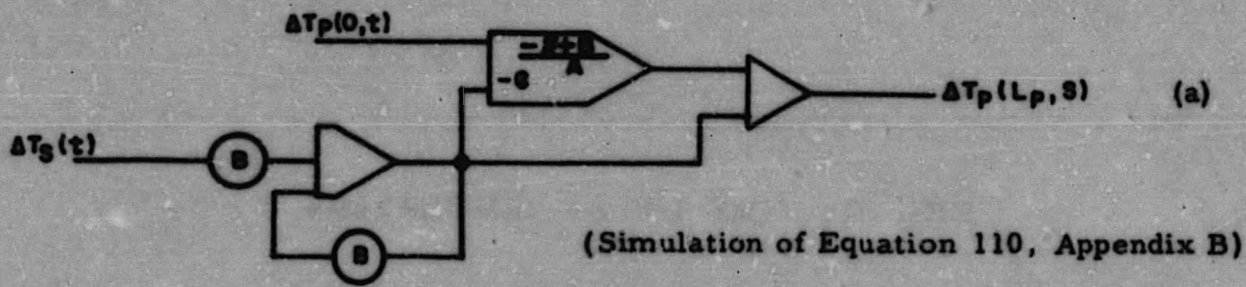FIG. 27: TIME DELAY SIMULATION

FIG. 28: BOILER SIMULATION DEVELOPMENT

$\Delta T_P(0,t)$

$\Delta T_P(L_p,S)$ (a)

$\Delta T_S(t)$

(Simulation of Equation 110, Appendix B)

$\Delta T_S(t)$

$\Delta T_P(L_p,t)$

$\Delta \bar{T}_P(t)$ (b)

$\Delta T_P(0,t)$

(Simulation of Equation 111, Appendix B)

$\Delta \bar{T}_P(t)$

$\Delta T_S(t)$ (c)

$\Delta P(t)$

(Simulation of Equation 112, Appendix B)
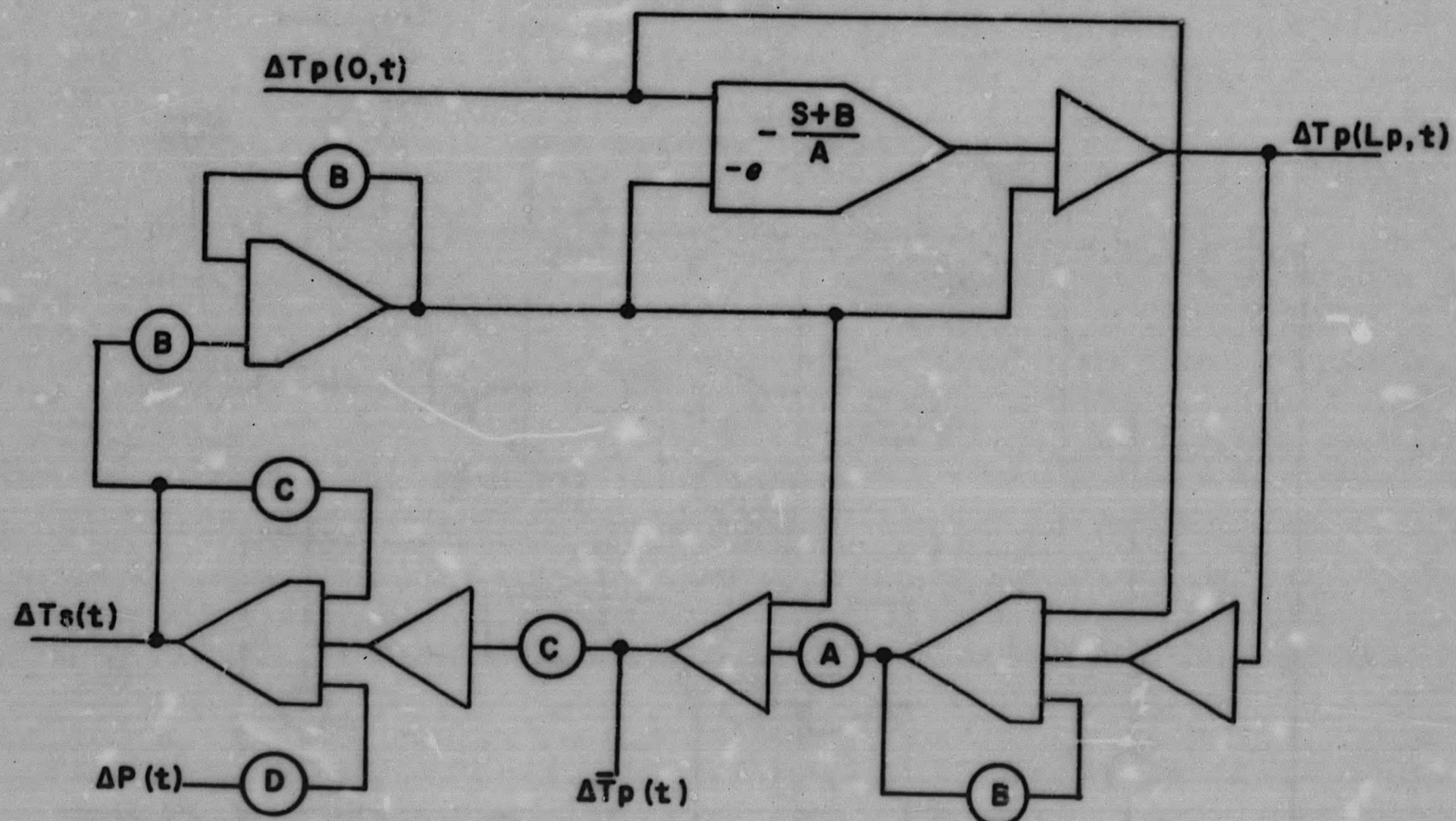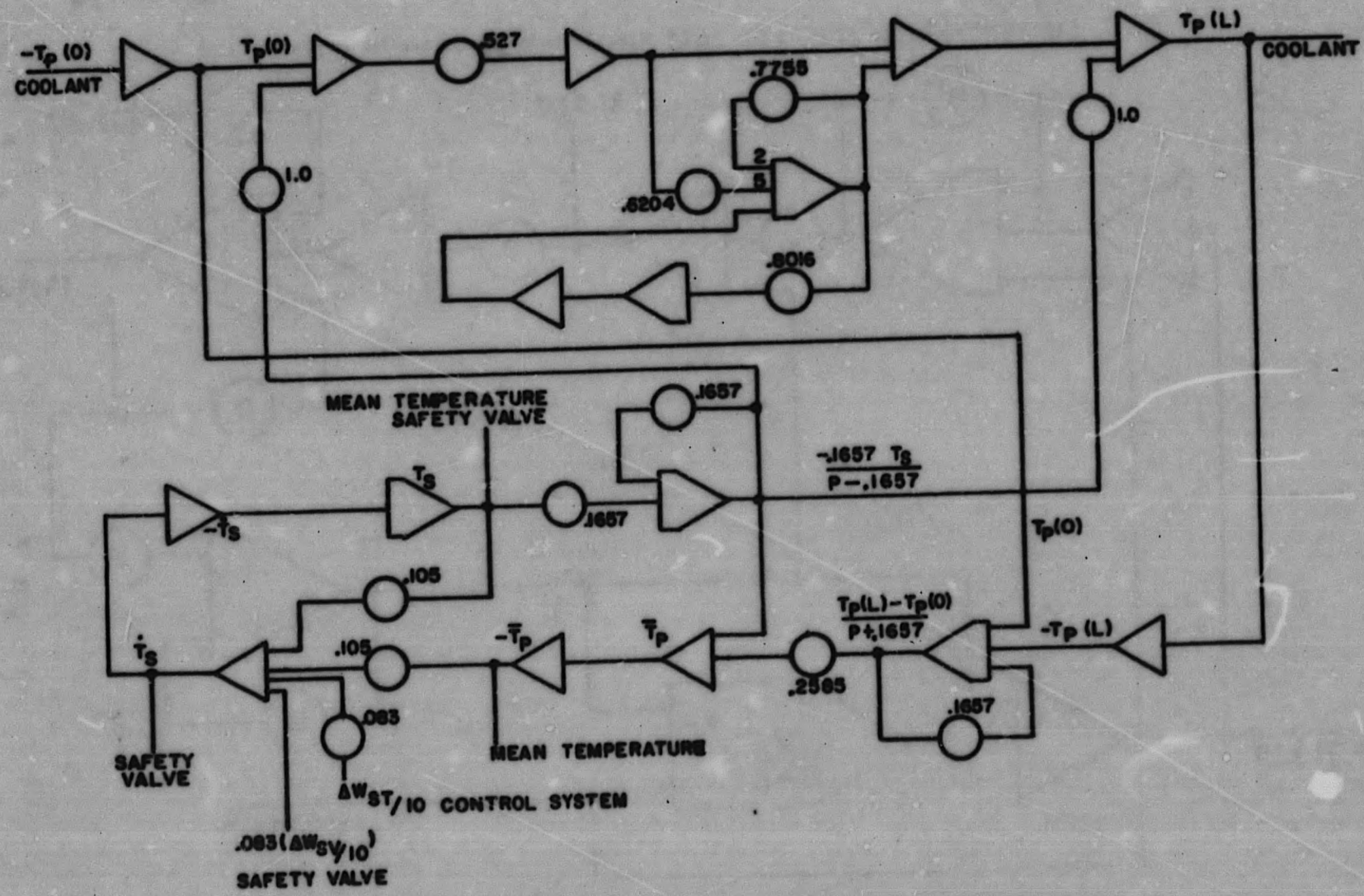
82
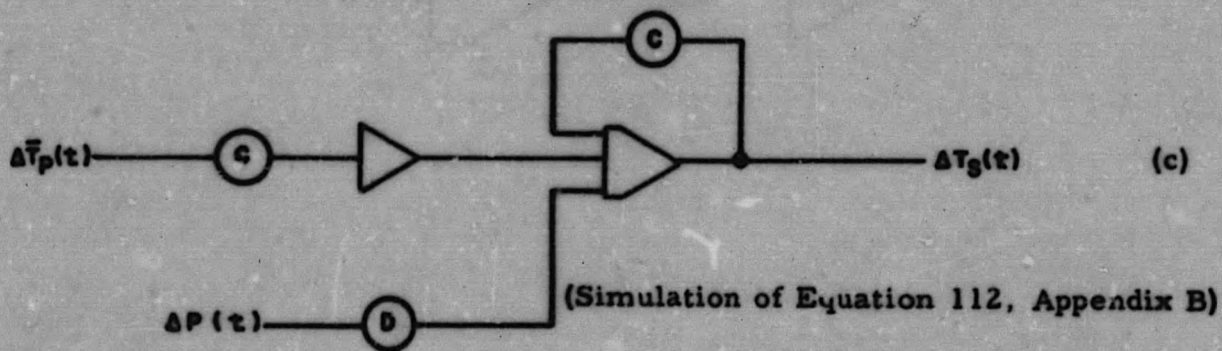
FIG. 29: BOILER SIMULATION

(Combined Simulation of Equations 110, 111, 112 — Appendix B)

FIG. 30: BOILER SIMULATION

(Simulation of Equations 118, 119, 120, 121 — Appendix B)